Department of Physics and Astronomy
Uppsala University

Master thesis

Effect of chameleons on the mass of a galaxy cluster

Isabel Roca Vich

Supervisor:	Dr. Martin Sahlén
Subject reader:	Prof. Ulf Danielsson
Examiner:	Dr. Andreas Korn

FYSAST
FYSMAS

Innehåll

Abstract

Chameleons are scalar fields coming from modified gravity theories and can be possible explanations for Dark Energy. They cause a fifth force and have a screening mechanism which allows this force to avoid solar system constraints. In this thesis, astrophysical consequences of the potential presence of the chameleon field will be studied. More precisely, the difference between the hydrostatical and the weak lensing mass of galaxy clusters due to the effect of the chameleon fifth force is discussed.

Sammanfattning

Chameleons är ett skalarfält som kommer från en modifierad teori om graviation och som möjligen kan förklara mörk energi. De orsakar en femte kraft och har en såkallad screenings mekanism som tillåter denna kraft att undvika experimentella gränser inom solsystemet. I denna avhandling studeras astrofysikaliska följder av en potentiell närvaro av ett chameleon fält. Mer exakt diskuteras skillnaden mellan den hydrostatiska och den svaga linsmassan hos galaxhopar som beror på en effekten som kommer av chameleonens femte kraft.

1 Introduction

In some simple modification of general relativity additional light scalar fields are introduced. Such a scalar field is expected to cause an additional force of Nature since it is coupling to matter. However, no experiment performed in our solar system was able to confirm the existence of such a fifth force [1]. The chameleon mechanism is a way of explaining this. A scalar field with a chameleon mechanism is generally called chameleon and has a mass which depends on the energy density of its surrounding. In this way, the fifth force caused by the chameleon is suppressed in the solar system and other dense regions since the chameleon's heavy mass restricts its interaction range.

This behavior is due to a special form of the chameleon self-interaction and the matter coupling potentials. Λ is the self-coupling constant of the chameleon and β describes the strength of the coupling to matter. This matter coupling is realized via conformal transformation of the metric. All this will be discussed in section [1.3]. In this thesis the effect of the chameleons on the mass of a galaxy cluster is investigated. More precisely, outside the galaxy cluster the chameleon field profile $\phi(r)$ can give an additional mass contribution which in turn A actually gives a difference between the cluster's hydrostatical and lensing mass.

This is due to the fact that the fifth force is affecting the density of the gas in a galaxy cluster when it is coupling to the gas components. An extra pressure gradient is caused which in turn balances the fifth force and leads to a denser gas distribution [4]. This effect is used to compare the X-ray profiles predicted by the use of the chameleon model because there will be a deviation of the hydrostatic mass of the galaxy cluster which can be measured by weak lensing. A good test for modified gravity is therefore to compare measurements from both gas and lensing masses. It is convenient to consider a galaxy cluster cluster since its gravitational lensing can be observed in regions of weak fifth force screening due to a cluster's size and mass distribution. Observational data from measurements of X-ray temperature and x-ray brightness is usually combined with weak lensing observations to constrain values of the chameleon parameters [4].

The first section is dealing with the underlying theory of the chameleon scalar field model, its screening mechanism, how the extra force is obtained and effective mass os the chameleon field. Besides, $f(R)$ gravity is treated since it is equivalent to the chameleon model for $\beta = 1/\sqrt{6}$.

In section [2], the method of obtaining the chameleon field profile and the extra mass M_ϕ produced by the fifth force F_ϕ are described. This is mainly based on a article by Terukina [4] and in that paperwhere they make investigations witg data from the Coma cluster which is a commonly used

example of glaxy cluster (see Figure 1). In section [3], plots of the chameleon profile and the extra mass are presented for different values of the chameleon and cluster parameters. These results are then discussed in the last section.

This thesis is mainly based on a analytic approach of the chameleon theory [1] and not on observational data. The numbers used as data in order to create plots for the functions presented to the figure in section [2] is based on two articles [4] and [19].

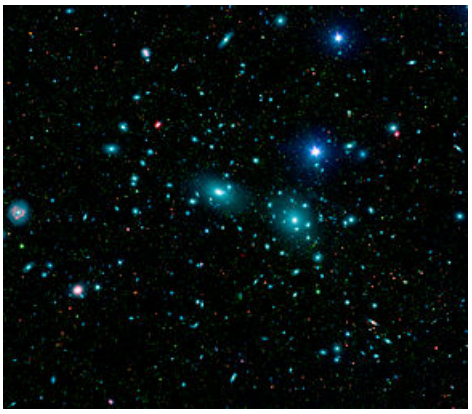

Figure 1: Picture of the Coma Cluster [22].

1.1 A brief explanation of some terms

In this thesis there could may be some new terms appearing which can be convenient to explain in more details.
The Euler-Lagrange equation of motion is a fundamental equation in the variation of calculus, it is a differential equation with a solution which describes the evolution of the system. This method is used to find a function that maximize and minimize a functional [11]. Poisson's equation is a partial differential equation containing a Laplace operator ∇^2.
The Poisson's equation used in this thesisi is an outcome from varying the action with respect to the scalar field ϕ where Laplace's equation is a special form of Poisson's equation.

In the chameleon model, an analogue to a freely moving test particle is often used in order to illustrate the general relativity's equation of motion (EOM) which is described by a geodesic equation. The geodesic equation describes the shortest way a freely moving particle would take while gravitational forces are acting on it in curved spacetime i.e. the particle is following a straight line. While Einstein's equation's describes how the mass or the source makes the spacetime curved where gravity is seen as an result of the

curved spacetime. In Newtonian gravity the mass density is the source of the field, while in general relativity, the stress-energy tensor is the source of the gravitational fields appearing in the Einstein field equations [12].
The stress-energy tensor is also often called the stress-energy-momentum tensor but also the energy-momentum tensor and are labeled with the letter T. This tensor describes the momentum, the energy flux and of course the energy density.

$$T^{\mu\nu} = \begin{pmatrix} T^{00} & T^{01} & T^{02} & T^{03} \\ T^{10} & T^{11} & T^{12} & T^{13} \\ T^{20} & T^{21} & T^{22} & T^{23} \\ T^{30} & T^{31} & T^{32} & T^{33} \end{pmatrix} \tag{1}$$

where T^{00} is the energy density while the three other components in the first column, as well as the first row, is the momentum density and the three components in the diagonal is the pressure while the rest of the 12 components are the momentum flux (the flux gives a description of the components energy and momentum flow) [12].
The Einstein Hilbert action is an action that will later appear in the chameleon principle in section 1.3. This is used in general relativity in order to generate the Einstein field equations which will be considered in more details in the Appendix [A.3].
The Einstein Hilbert action is often described in the Einstein or in the Jordan frame. These two frames are equivalent to each other because they describe the same physics and are related through a conformal transformation of the metric which re-scales all the length scales [10]. The conformal transformation used here inclueds the matter fields $\psi_m^{(i)}$ (each matter field couples to the metric $g_{\mu\nu}^{(i)}$) in the matter action S_m. This happens in the Jordan frame where the scalar field ϕ couples to matter via a conformal transformation $e^{\frac{2\beta_i\phi}{M_{Pl}}}$ of the Einstein frame metric [1].
Another thing often used here is the so called Yukawa potential which is a screened Coulomb potential of the form:

$$-g^2\frac{e^{-kmr}}{r} \tag{2}$$

where g is the amplitude of the potential, k is a scaling constant, r is the radial distance and m is the mass of the particle. The potential is negative and montonically increasing with r indicating that the force is positive [3]. The reason why it is convenient to use a Yukawa potential is because it is

suppressing the contribution from a massive object's core (like a galaxy cluster for example). The exterior field profile $\phi(r)$ will only contain contribution from the massive object's thin-shell [2], for more about the field profile of an massive object, see section A.11.

1.2 Dark energy

The present Universe is expanding at an accelerated rate [5]. In lack of names and knowledge, this phenomenon that drives the expansion of space and time forward is called dark energy (DE). We know that particles are force carriers but it is the forces which are interacting over larger scales which cause the expansion of the universe. This dark energy has a negative pressure and works against gravity. A common candidate for dark energy is the cosmological constant, usually labeled as Λ which gives the value of the energy density of vacuum of space. The concept behind this is that dark energy is spread out and clusters in a slower way than matter. Λ is the vacuum energy density meaning that Λ is positive and that the pressure P is negative and a negative pressure is driving the acceleration of the universe forward. The equation of state (EOS) of the cosmological constant is the ratio between the pressure and the energy density which in this case, have the value of $\omega = -1$. This tells us how the energy is distributed per volume unit in the universe with a constant energy density in space and time. The problem with the cosmological constant is that its observed value is much smaller than predicted by QFT calculations. The Einstein equation $R_{\mu\nu} - \frac{1}{2}g_{\mu\nu}R + \Lambda g_{\mu\nu} = 8\pi G T_{\mu\nu}$ follows from the action

$$S = \frac{1}{16\pi G}\int \mathrm{d}^4x\sqrt{-g}(R - 2\Lambda) + S_m \tag{3}$$

of the cosmological constant dark matter model, ΛCDM, through the action principle i.e. that $\delta S = 0$. S_m is the action of matter.

If the problem with the cosmological constant is solved in such a way that it is vanishing completely one has to try other models in order to explain dark energy. There are two ways. One is with modified matter through the energy momentum tensor $T_{\mu\nu}$ where the RHS of the Einstein equation contains an exotic source of matter with negative pressure. The other opption is by modified gravity when instead the LHS of the Einstein equation containing the Einstein tensor $G_{\mu\nu}$ is modified as and one example of this is the chameleons.

The first suggestion is the quintessence model which has a scalar field Q with the difference that its EOS is changing dynamically with time and the energy density does not need to be small compared to the matter and

radiation density at a early stage of the Universe's evolution. The action is an integral containing the canonical scalar field Q with a potential V. The field is frozen at the potential's maximum during the period when the fields mass $m_q < H$, where H is the Hubble parameter which tells us how fast galaxies are moving away from us i.e. it is dependent on the distance. The label q is referring to the quintessence. The field will start to roll down its potential when m_q is approximatley H_0, as it is today. It can be repulsive or attractive depending on the ratio between the kinetic energy and the potential of the scalar field which gives the value of its EOS

$$\omega_q = \frac{P_q}{\rho_q} \tag{4}$$

$$\frac{P_q}{\rho_q} = \frac{\frac{1}{2}\dot{Q}^2 - V(Q)}{\frac{1}{2}\dot{Q}^2 + V(Q)} \tag{5}$$

so ω_q is varying as a function of time.

Many quintessence models contain something called tracker solutions. This tracking behavior partially solves the cosmological constant problem where the scalar field $Q : s$ density is following the evolution of (but it is still less than) the radiation density until a stage in the evolution of the Universe where the radiation and matter density were equal and this is why Q is acting like dark energy. The field depends on the density of matter and so when the Universe reaches an era of Dark Energy domination the field will start to follow its own energy density.

When it comes to the energy density in the Universe of today, it is similar for DE as it is for DM. This can be a clue that there is a connection between them. There have been many different suggested couplings between DM and DE where f(R) gravity is one of them which will be treated in section 1.5.

One possibility is to consider this interaction between the quintessence field Q and DM.

The interaction between the scalar field and non-relativistic matter is given by:

$$\nabla_\mu T^\mu_{\nu(Q)} = -\beta T_M \nabla_\nu Q \tag{6}$$

$$\nabla_\mu T^\mu_{\nu(M)} = +\beta T_M \nabla_\nu Q \tag{7}$$

where the energy momentum tensors are for both Q and matter. T_M is traceless for the radiation part ($\rho_M = 3P_M$) while the trace of the matter

fluid is $T_M = -\rho_M + 3P_M$. The coupling dependent term in equation (6) and (7) vanishes while the matter is coupled to the scalar field Q. If the baryons are not coupled they are free and follow a geodesic and can then be compared to observations because nothing else except gravitation is affecting them over larger scales and the frame in that the baryons are following the geodesic is a physical frame. If they instead are coupled, the physical frame must be obtained through a so called conformal transformation which will be discussed later in section 1.7.

The Lagrangian for coupled quintessence is $L_q = \frac{1}{2}\dot{Q}^2 - V + L_{int}$ where the last part is giving rise to the interacting energy momentum tensor in equation (6) and (7). V is an exponential. If dark matter is coupling to the dark energy as in the quintessence model, the dark energy would affect the expansion of the universe in the past as well as the formation of large structures.

1.3 Chameleons

Chameleons are a scalar theory and the underlying concept behind the chameleon mechanism is to make the chameleon's mass, density dependent [8] this is done by considering scalar fields which are minimally coupled to matter. The scalar field has a mass which depends on the environmental mass density [6] such that the free propagation of the scalar field is stopped in dense environments [8]. This mechanism is usually formulated in the Einstein conformal frame where the coupling between the scalar field and the scalar curvature is minimal [6]. Furthermore, the field profile of the scalar field is dependent on the enviormental mass density. Later in section 1.9, a Poisson equation will be obtained from varying the Einstein-Hilbert action with respect to the scalar field ϕ and it will be convenient to generalize the left hand side (LHS) of this Poisson equation into an effective potential. At that stage, everything boils down to choose the right values on the potential in order to obtain larger values of the scalar field's mass in dense regions [8].

A simple example of how the chameleon mechanism suppresses the scalar field is to consider a test particle in the Einstein frame. The geodesic equation is modified due to the coupling between the scalar field and the matter fields where the acceleration of the test particle is obtained from the geodesic equation. For scales smaller than the Compton wavelength m^{-1}, the Yukawa suppression (see section 1.1 for Ykuawa Potential) can be neglected and the particle will then only feel a modified Newton potential Φ. At scales larger than the Compton wavelength the test particle will feel unmodified gravity due to the Yukawa suppression which makes sure that the scalar field will not propagate freely. In other words, if the mass of the chameleons is large

in dense environments the scalar field will not propagate above the Compton wavelength of the chameleon m^{-1} where m is the mass of the chameleon., i.e. the scalar field is considered to be short ranged. The fifth force which is produced by the scalar field will then be suppressed. The mass is instead smaller in low density regions and the fifth force will not be suppressed and will in turn modify the gravity, i.e. the field is long ranged [8].

1.4 Chameleons and Dark Energy

Here, the scalar field of the chameleon ϕ is a modified case of the quintessence model and it is coupling to non-relativistic matter which gives rise to a fifth force [5]. From now on, the scalar field of the chameleon will be labeled with ϕ but it is in fact the same as the scalar field of the quintessence model Q. The chameleon mechanism is based on that the coupled quintessence field effective mass is different depending on the density of the environment. The coupling to the matter give rise to a frozen field, an extremum for the field potential to sit on. In other words, if the region is very dense, the field will possess a heavy mass at the potentials minimum and it cannot propagate freely. The field is starting to evolve in a thin shell of a massive object where the action integral is similar to the coupled quintessence model and the field is starting to roll along its potential.

However in some modified gravity theories e.q. f(R) gravity, the cosmological constant is generated by the theory. To see the connection between the chameleons and Dark Energy one starts with the Lagrangian density

$$\mathcal{L} = -\frac{1}{2}(\partial\phi)^2 - \frac{\lambda}{4!}\phi^4 - \rho\frac{\phi}{M_{Pl}} \tag{8}$$

and the constant backround value for chameleon $< \phi >=: \phi_0 \neq 0$ and $\phi =: \phi_0 + \delta\phi$ where $\delta\phi$ is a fluctuation. The Lagrangian can now be written as:

$$\mathcal{L} = -\frac{1}{2}(\partial\delta\phi)^2 - \frac{\lambda}{4!}(\phi_0 + \delta\phi)^4 - \frac{\rho}{M_{Pl}}(\phi_0 + \delta\phi) \tag{9}$$

and evaluate the second term

$$-\frac{\lambda}{4!}(\phi_0 + \delta\phi)^4 = -\frac{\lambda}{4!}(\phi_0^4 + 4\phi_0^3\delta\phi + 6\phi_0^2\delta\phi^2 + 4\phi_0\delta\phi^3 + \delta\phi^4) \tag{10}$$

where the first term $\frac{\lambda}{4!}\phi_0^4$ is a potential cosmological constant term.

1.5 $f(\mathcal{R})$ gravity

$f(\mathcal{R})$ gravity is a modification of Einstein's theory of gravity. It is equivalent to a scalar tensor theory with an extra scalar degree of freedom added. The

Ricci scalar is replaced by an arbitrary function of the Ricci scalar in the Einstein-Hilbert action [2]. This model can manifest a so called chameleon screening which will be expalined more in section 1.7.
The action of this type of modified gravity model is the modified Einstein-Hilbert action:

$$S = \frac{M_{Pl}^2}{2}\int \mathrm{d}^4x\sqrt{-g}\Big(\mathcal{R} + f(\mathcal{R})\Big) + S_m[g_{\mu\nu}, \psi], \tag{11}$$

where $\mathcal{R}$ is the Ricci scalar and it is also assumed that the matter field ψ couples minimally to the metric $g_{\mu\nu}$ and the index of letter m in S is referring to matter. It can also be written as:

$$S = \frac{M_{Pl}^2}{2}\int \mathrm{d}^4x\sqrt{-g}\Big(\mathcal{R} + f(\Phi) + \frac{\mathrm{d}f}{\mathrm{d}\Phi}(\mathcal{R} - \Phi)\Big) + S_m[g_{\mu\nu}, \psi]. \tag{12}$$

Where $\Phi = \mathcal{R}$ and $F(\mathcal{R}) \equiv \frac{\mathrm{d}f}{\mathrm{d}\Phi} = \frac{\mathrm{d}f}{\mathrm{d}\mathcal{R}}$. Φ is like an auxiliary field because there are no time derivatives included in its equation of motion (EOM) and it is therefore non-dynamical i.e. it does not have a second derivative of Φ. However, by varying the action in equation (11) with respect to the metric $g^{\mu\nu}$ gives the modified Einstein equation (see [A.3]):

$$(1 + F(\mathcal{R}))\mathcal{R}_{\mu\nu} - \frac{1}{2}\Big(\mathcal{R} + f(\mathcal{R}) - 2\Box F(\mathcal{R})\Big)g_{\mu\nu} - \nabla_\mu\nabla_\nu F(\mathcal{R}) = \frac{1}{M_{Pl}^2}T^m_{\mu\nu} \tag{13}$$

and the trace of this equation above is

$$3\Box F(\mathcal{R}) - \mathcal{R} - 2f(\mathcal{R}) + F(\mathcal{R})\mathcal{R} = -\frac{1}{M_{Pl}^2}T. \tag{14}$$

Considering the trace of this expression above, it can be seen as an equation for the scalar degree of freedom (DOF) $F(\mathcal{R})$:

$$\Box F(\mathcal{R}) = \frac{1}{3}\Big(\mathcal{R} + 2f(\mathcal{R}) - F(\mathcal{R})\mathcal{R} + \frac{1}{M_{Pl}^2}T\Big) \equiv \frac{\mathrm{d}V_{eff}}{\mathrm{d}F(\mathcal{R})}. \tag{15}$$

V_{eff} is the effective potential. Later, this will be treated in more details when it comes to vary the action for a scalar field with respect to ϕ in section 1.7. Now, taking the second derivative of the expression above;

$$\frac{1}{3}\Big(\frac{\mathrm{d}\mathcal{R}}{\mathrm{d}F(\mathcal{R})} + 2\frac{\mathrm{d}f(\mathcal{R})}{\mathrm{d}F(\mathcal{R})}\Big) \tag{16}$$

$$m_{eff}^2(F(\mathcal{R})) = \frac{1}{3}\bigg((1 + F(\mathcal{R})/\frac{\mathrm{d}^2 f}{\mathrm{d}\mathcal{R}^2} - \mathcal{R}\bigg) \tag{17}$$

which is the effective mass of the scalar $F(\mathcal{R})$ and using a conformal transformation

$$\tilde{g}_{\mu\nu} = \bigg(1 + \frac{\mathrm{d}f}{\mathrm{d}\Phi}\bigg) g_{\mu\nu} \tag{18}$$

gives the scalar field:

$$\phi = -\sqrt{\frac{3}{2}} M_{Pl} \log\bigg(1 + \frac{\mathrm{d}f}{\mathrm{d}\Phi}\bigg) \tag{19}$$

which leads to the action:

$$S = \int \mathrm{d}^4x\sqrt{-\tilde{g}}\bigg(\frac{M_{Pl}}{2}\tilde{\mathcal{R}} - \frac{1}{2}\tilde{g}^{\mu\nu}\partial_\mu\phi\partial_\nu\phi - V(\phi)\bigg) + S_m[e^{-\sqrt{\frac{2}{3}}\phi/M_{Pl}}\tilde{g}_{\mu\nu}, \psi]. \tag{20}$$

$\tilde{\mathcal{R}}$ is the Ricci scalar in the Jordan frame. Defining the conformal factor $A^2(\phi) = e^{-\sqrt{\frac{2}{3}}\phi/M_{Pl}}$ with an appropriate value on the potential $V(\phi)$ will denote a chameleon screening [2]. For more information about $f(\mathcal{R})$ gravity see the Appendix sections [A.2] and [A.3].

1.6 Linking $f(\mathcal{R})$ gravity to a scalar-tensor theory

The purpose here is to see if $f(\mathcal{R})$ obtained in the previous section [1.5] is equivalent with a scalar-tensor theory and finally get an expression for the action of a scalar field which will be used later for the Chameleon's scalar field. The steps belov are based on the article [16]. Lets go back and considering equation (11) but now, only considering the $f(\mathcal{R})$-part.

$$S = \frac{M_{Pl}^2}{2}\int \mathrm{d}^4x\sqrt{-g}f(\mathcal{R}) + S_m[g_{\mu\nu}, \psi]. \tag{21}$$

Just like in the previous section this will result in the modified Einstein equation:

$$\bigg(F(\mathcal{R})\mathcal{R}_{\mu\nu} - \frac{1}{2}f(\mathcal{R}) - \Box F(\mathcal{R})\bigg)g_{\mu\nu} + \nabla_\mu\nabla_\nu F(\mathcal{R}) = \frac{1}{M_{Pl}^2}T^m_{\mu\nu} \tag{22}$$

The action above has to be dynamically equivalent to the following action by adding a new field χ:

$$\delta S = \frac{M_{Pl}^2}{2}\int \mathrm{d}^4x\sqrt{-g}\bigg(f(\chi) + F(\chi)(\mathcal{R} - \chi)\bigg) + S_m[g_{\mu\nu}, \psi]. \tag{23}$$

This is done by varying the action with respect to χ.

$$\delta S = \frac{M_{Pl}^2}{2}\int \mathrm{d}^4x\sqrt{-g}\Big(f(\delta\chi) + F(\delta\chi)\mathcal{R} - F(\delta\chi)\chi - F(\chi)\delta\chi\Big) + S_m[g_{\mu\nu},\psi]. \tag{24}$$

(Keep in mind that $F(\mathcal{R}) = f'(\mathcal{R})$ from the previous section).

$$S = \frac{M_{Pl}^2}{2}\int \mathrm{d}^4x\sqrt{-g}\Big(F(\chi) + F'(\chi)\mathcal{R} - F'(\chi)\chi - F(\chi)\Big)\delta\chi + S_m[g_{\mu\nu},\psi]. \tag{25}$$

with the condition that the variation vanish i.e. $\delta S/\delta\chi = 0$ and concluding that:

$$F'(\chi)\mathcal{R} - F'(\chi)\chi = 0 \tag{26}$$

where $F'(\chi) = f''(\chi)$ meaning that if $f''(\chi) \neq 0$ then $\mathcal{R} = \chi$ and by plugging this back into the action in equation (23) gives the first action in equation (21). Let $\Phi = F(\chi)$ and put this into the action in equation (23) as well as identifying the rest of the terms as a potential $V(\Phi) = \Phi\chi - f(\chi)$ results in:

$$S = \frac{M_{Pl}^2}{2}\int \mathrm{d}^4x\sqrt{-g}\Big(\Phi\mathcal{R} + V(\Phi)\Big) + S_m[g_{\mu\nu},\psi]. \tag{27}$$

Differentiating this with respect to Φ and if $\chi = \mathcal{R}$ would give $V'(\Phi) = \mathcal{R}$, $\Phi = F(\mathcal{R})$ and $f(\mathcal{R}) = \Phi\mathcal{R} - V(\Phi)$ then the Einstein equation (22) can be written as

$$\Phi\mathcal{R}_{\mu\nu} - \frac{1}{2}g_{\mu\nu}(\Phi\mathcal{R} - V(\Phi)) - g_{\mu\nu}\Box\Phi + \nabla_\mu\nabla_\nu\Phi = \frac{1}{M_{Pl}^2}T^m_{\mu\nu} \tag{28}$$

or

$$\Phi(\mathcal{R}_{\mu\nu} - \frac{1}{2}g_{\mu\nu}\mathcal{R}) = -\frac{1}{2}g_{\mu\nu}V(\Phi)) + g_{\mu\nu}\Box\Phi - \nabla_\mu\nabla_\nu\Phi + \frac{1}{M_{Pl}^2}T^m_{\mu\nu}. \tag{29}$$

The conformal transformation is $\tilde{g}^{\mu\nu} = \Phi g^{\mu\nu}$ and $\sqrt{-g} = \Phi^{-2}\sqrt{-\tilde{g}}$;

$$\mathcal{R} = \Phi\Big(\tilde{\mathcal{R}} + 3\big(\frac{\Box\Phi}{\Phi} - \frac{3}{2}\big(\frac{\nabla\Phi}{\Phi}\big)^2\big)\Big) \tag{30}$$

This can be plugged back into equation (27)

$$
\begin{aligned}
S &= \frac{M_{Pl}^2}{2}\int \mathrm{d}^4x\Phi^{-2}\sqrt{-\tilde{g}}\Phi^2\bigg(\tilde{\mathcal{R}}+3\frac{\Box\Phi}{\Phi}-\frac{9}{2}\big(\frac{\nabla\Phi}{\Phi}\big)^2-\frac{V(\Phi)}{\Phi^2}\bigg)\\
&\quad +S_m[\Phi^{-1}\tilde{g}_{\mu\nu},\psi]\\
&= \frac{M_{Pl}^2}{2}\int \mathrm{d}^4x\sqrt{-\tilde{g}}\bigg(\tilde{\mathcal{R}}+3\frac{\Box\Phi}{\Phi}-\frac{9}{2}(\nabla\log\Phi)^2-\frac{V(\Phi)}{\Phi^2}\bigg)\\
&\quad +S_m[\Phi^{-1}\tilde{g}_{\mu\nu},\psi]. \qquad (31)
\end{aligned}
$$

The steps done in equation (31) can be found in Appendix [A.3.1]. If $\Phi = e^{2\beta\phi/M_{Pl}}$ and defining the potential term as $\tilde{V}(\Phi) = V(\Phi)/M_{Pl}^2\Phi^2$ which is $\tilde{V}(\Phi) = \frac{\Phi\chi - f(\chi)}{M_{Pl}^2\Phi^2} = \frac{e^{2\beta\phi/M_{Pl}}(\chi-f(\chi))}{M_{Pl}^2 e^{2\beta\phi/M_{Pl}}}$ and $\mathcal{R} = \chi$. Then, this potential can be written as $\tilde{V}(\Phi) = \frac{\Phi\mathcal{R}-f(\mathcal{R})}{M_{Pl}^2\Phi^2}$. This shows that this potential depends on $f(\mathcal{R})$ and there is a inverse power of Φ here. In $f(R)$ gravity using that the coupling term $\beta = 1/\sqrt{6}$ in the metric formalism [5], will result in the action of a scalar-tensor theory which also can be found in the Appendix [A.3]:

$$
= \int \mathrm{d}^4x\sqrt{-\tilde{g}}\big(\frac{M_{Pl}^2}{2}\tilde{\mathcal{R}}-\frac{1}{2}(\partial\phi)^2-\tilde{V}(\phi)\big)+S_m[e^{-2\beta\phi/M_{Pl}}\tilde{g}_{\mu\nu},\psi]. \qquad (32)
$$

$\mathcal{L}$ is dynamically equivalent to $\mathcal{L}\sqrt{-g}$ because the term $\sqrt{-\tilde{g}}$ is constant and it does not change the dynamics [16].

1.7 The Chameleon's scalar field ϕ

The scalar field of the chameleon is density dependent and in order to work out a field profile it is good to get a deep understanding for the basics behind this theory i.e. the derivation from varying the Einstein-Hilbert action with respect to ϕ. In the end via the Euler-Lagrangian equation the outcome is the equation of motion i.e. a Poisson's equation. Furthermore, by identifying the potential part in a general Lagrangian for a scalar field and comparing it to the obtained Poisson's equation, it is possible to get a picture of how the ϕ-force looks like. The derivation below is done to explain the steps in more detail in order to get a deeper understanding of why this method is used when it comes to obtain density dependent field profiles.
The Einstein-Hilbert action is [1]

$$
S = \int \mathrm{d}^4x\sqrt{-g}\bigg(\frac{M_{Pl}^2}{2}\mathcal{R}-\frac{1}{2}(\partial\phi)^2-V(\phi)\bigg)-S_m \qquad (33)
$$

where

$$S_m = \int \mathrm{d}^4x \mathcal{L}_m(\psi_m^{(i)}, g_{\mu\nu}^{(i)}) \tag{34}$$

and g is the determinant of the metric $g_{\mu\nu}$. $M_{Pl} \equiv (8\pi G)^{-\frac{1}{2}}$, $\mathcal{R}$ is the Ricci scalar, S_m is the matter action, a functional of the Jordan-frame metric and $\psi_m^{(i)}$ are matter fields. Each matter field couples to a metric $g_{\mu\nu}^{(i)}$ and the scalar field ϕ couples to matter via a conformal transformation $e^{\frac{2\beta_i\phi}{M_{Pl}}}$ of the Einstein frame metric

$$g_{\mu\nu}^{(i)} = e^{\frac{2\beta_i\phi}{M_{Pl}}} g_{\mu\nu}. \tag{35}$$

$V(\phi)$ is a self interaction potential and is given as a Ratra-Peebles inverse power law potential [1]

$$V(\phi) = \frac{M^{4+n}}{\phi^n} \tag{36}$$

This type of potential is used in diffrent theories. For example, in the quintessence model [20] mentioned earlier in section [1.2] which is used to explain the expansion of the universe. Where a new scalar field Q, slowly rolling along its potential. This scalar field needs to have this form of potential in order to avoid initial condition problems appearing when the values of the ratio between the matter and the energy densities has to be put to an infinitesimal value at an early stage of the universe evolution so that the values of these densities are consistent today [20]. In that sense, the chameleon field is linked and gives rise to the extra gravitational force via the coupling β in the extra term of the potential above. As an example, if $\beta = 0$ means that there would only be an ordinary gravitational field, i.e. ordinary quintessence. In addition, this power law potential is also used in a supersymmetric fermion condensate model [14].

The Lagrangian is

$$L(t) = \int \mathrm{d}^3x \mathcal{L}(\phi, \partial^\mu\phi) \tag{37}$$

where $\mathcal{L}$ is the Lagrangian density.
The action can for a general case be written as

$$\begin{aligned} S &= \int_{\mathrm{t_1}}^{\mathrm{t_2}} \mathrm{d}t \int \mathrm{d}^3x \mathcal{L} = \int \mathrm{d}^4x \mathcal{L} \\ &= \int \mathrm{d}^4x \sqrt{-g}[-\frac{1}{2}(\partial\phi)^2 - V(\phi)] - \int \mathrm{d}^4x \mathcal{L}_m(\psi_m^{(i)}, g_{\mu\nu}^{(i)}). \end{aligned} \tag{38}$$

The Euler-Lagrange equation is obtained by taking the variation of the action with respect to ϕ in a general case just to show the underlying theory behind it

$$\begin{aligned} \delta S &= \int \mathrm{d}^4x \left[\frac{\partial \mathcal{L}}{\partial \phi}\delta\phi + \frac{\partial \mathcal{L}}{\partial(\partial^\mu \phi)}\delta(\partial^\mu \phi) \right] \\ &= \int \mathrm{d}^4x \left[\frac{\partial \mathcal{L}}{\partial \phi}\delta\phi + \frac{\partial \mathcal{L}}{\partial(\partial^\mu \phi)}\frac{\partial \delta\phi}{\partial x_\mu} \right]. \end{aligned} \tag{39}$$

Integrating the second term by parts leads to

$$\int \mathrm{d}^4x \frac{\partial \mathcal{L}}{\partial(\partial^\mu \phi)}\frac{\partial \delta\phi}{\partial x_\mu} = \int \mathrm{d}^4x \left[\partial^\mu \left(\frac{\partial \mathcal{L}}{\partial(\partial^\mu \phi)}\delta\phi \right) - \partial^\mu \frac{\partial \mathcal{L}}{\partial(\partial^\mu \phi)}\delta\phi \right] \tag{40}$$

Where the second term is put back together with equation (38)

$$\delta S = \int \mathrm{d}^4x \left[\left(\frac{\partial \mathcal{L}}{\partial \phi} - \partial^\mu \frac{\partial \mathcal{L}}{\partial(\partial^\mu \phi)} \right) \delta\phi + \partial^\mu \left(\frac{\partial \mathcal{L}}{\partial(\partial^\mu \phi)}\delta\phi \right) \right]. \tag{41}$$

It is only the path which is varying and not the endpoints. The last term will vanish after integration due to $\delta\phi(\mathrm{t}_1) = \delta\phi(\mathrm{t}_2)$ which leads to

$$\delta S = \int \mathrm{d}^4x \left(\frac{\partial \mathcal{L}}{\partial \phi} - \partial^\mu \frac{\partial \mathcal{L}}{\partial(\partial^\mu \phi)} \right) \delta\phi. \tag{42}$$

For any small changes $\delta\phi$, $\delta S = 0$ which is the stationary value. Finally, the Euler-Lagrange equation is [9]:

$$\frac{\partial \mathcal{L}}{\partial \phi} - \frac{\partial}{\partial x_\mu}\left(\frac{\partial \mathcal{L}}{\partial(\partial^\mu \phi)} \right) = 0. \tag{43}$$

Next, the specific action in equation (33) is varied with respect to ϕ in order to find its equation of motion. To make it easier, the first integral in equation (33) which contains two terms will be treated first

$$\delta \int \mathrm{d}^4x \sqrt{-g}(-\frac{1}{2}(\partial\phi)^2 - V(\phi)). \tag{44}$$

This is done by making an infinitesimal variation $\delta\phi$, using the derivation above and demanding that the corresponding variation of the action is $\delta S = 0$

$$\delta S = \int \mathrm{d}^4x \sqrt{-g} \Big[-\frac{1}{2}\partial_\mu \delta\phi \partial^\mu \phi - \frac{1}{2}\partial^\mu \phi \partial_\mu \delta\phi - V(\delta\phi) \Big]. \tag{45}$$

The two first terms are integrated by parts (just like above)

$$\delta S = \int \mathrm{d}^4x\sqrt{-g}(\partial^\mu\partial_\mu\phi - V^{'}(\phi))\delta\phi. \tag{46}$$

$\partial^\mu\partial_\mu\phi$ can be rewritten as $\partial^\mu\partial_\mu\phi = \partial^2\phi$ and the first integral can be expressed as:

$$\delta S = \int \mathrm{d}^4x\sqrt{-g}(\partial^2\phi - V^{'}(\phi))\delta\phi \tag{47}$$

finally the expression for the first integral is:

$$\delta S = \int \mathrm{d}^4x\sqrt{-g}\big(\partial^2\phi - V^{'}(\phi)\big). \tag{48}$$

Varying the second integral with respect to ϕ from equation (33) lead to

$$\delta \int \mathrm{d}^4x\mathcal{L}_m(\psi_m^{(i)}, g_{\mu\nu}^{(i)}) = \int \mathrm{d}^4x\frac{\partial\mathcal{L}_m}{\partial\phi}\delta\phi \tag{49}$$

$$= \int \mathrm{d}^4x\frac{\partial\mathcal{L}_m}{\partial g_{\mu\nu}^{(i)}}\frac{\partial g_{\mu\nu}^{(i)}}{\partial\phi}\delta\phi. \tag{50}$$

Each matter field $\psi_m^{(i)}$ in the Einstein-frame, couples to each metric $g_{\mu\nu}^{(i)}$ so that the metric $g_{\mu\nu}^{(i)}$ re-scale as:

$$g_{\mu\nu}^{(i)} = e^{\frac{2\beta_i\phi}{M_{Pl}}}g_{\mu\nu}. \tag{51}$$

Replace this expression into equation (50) which will give the result:

$$\int \mathrm{d}^4x\frac{\partial\mathcal{L}_m}{\partial g_{\mu\nu}^{(i)}}(\frac{\partial}{\partial\phi}e^{\frac{2\beta_i\phi}{M_{Pl}}}g_{\mu\nu})\delta\phi = \int \mathrm{d}^4x\frac{\partial\mathcal{L}_m}{\partial g_{\mu\nu}^{(i)}}(\frac{2\beta_i\phi}{M_{Pl}}e^{\frac{2\beta_i\phi}{M_{Pl}}}g_{\mu\nu})\delta\phi \tag{52}$$

$$= \int \mathrm{d}^4x\frac{\partial\mathcal{L}_m}{\partial g_{\mu\nu}^{(i)}}(\frac{2\beta_i\phi}{M_{Pl}}g_{\mu\nu}^{(i)})\delta\phi. \tag{52}$$

Put the first integral equation (44) together with this second integral equation (52):

$$\delta S = \int \mathrm{d}^4x\sqrt{-g}(\partial^2\phi - V^{'}(\phi))\delta\phi - \int \mathrm{d}^4x\frac{\partial\mathcal{L}_m}{\partial g_{\mu\nu}^{(i)}}(\frac{2\beta_i\phi}{M_{Pl}}g_{\mu\nu}^{(i)})\delta\phi. \tag{53}$$

The trace is $g^{(i)} = e^{\frac{8\beta_i\phi}{M_{Pl}}} g$, dividing the second integral with $\frac{1}{\sqrt{-g}} = \frac{1}{\sqrt{-g^{(i)}}} e^{\frac{4\beta_i\phi}{M_{Pl}}}$ and only considering the second integral gives:

$$\sum_i \frac{2\beta_i}{M_{Pl}} \frac{1}{\sqrt{-g}} \frac{\partial \mathcal{L}_m}{\partial g^{\mu\nu}_{(i)}} g^{\mu\nu}_{(i)} = \sum_i \frac{2\beta_i}{M_{Pl}} \frac{e^{\frac{4\beta_i\phi}{M_{Pl}}}}{\sqrt{-g^{(i)}}} \frac{\partial \mathcal{L}_m}{\partial g^{\mu\nu}_{(i)}} g^{\mu\nu}_{(i)}. \tag{54}$$

At this stage there are terms appearing in this equation which can be replaced by the stress-energy tensor, see Appendix [A.6] for more information about the stress-energy tensor:

$$T^{(i)}_{\mu\nu} = \frac{2}{\sqrt{-g^{(i)}}} \frac{\delta \mathcal{L}_m}{\delta g^{(i)}_{\mu\nu}}. \tag{55}$$

Put $T^{(i)}_{\mu\nu}$ into equation (54) to finally get an expression for the second integral:

$$S_m = \sum_i \frac{\beta_i}{M_{Pl}} e^{\frac{4\beta_i\phi}{M_{Pl}}} T^{(i)}_{\mu\nu} g^{\mu\nu}_{(i)}. \tag{56}$$

Finally, when both the first and the second integral are done it is time to add them up by taking the result from the first integral in equation (48) as well as the result from the second one in equation (56) which leads to the Poisson equation

$$\nabla^2\phi = V^{'}(\phi) - \sum_i \frac{\beta_i}{M_{Pl}} e^{\frac{4\beta_i\phi}{M_{Pl}}} g^{\mu\nu}_{(i)} T^{(i)}_{\mu\nu}. \tag{57}$$

The trace of the Jordan-frame metric stress tensor is $\tilde{T} = g^{\mu\nu}_{(i)} \tilde{T}^{(i)}_{\mu\nu}$. This tensor $\tilde{T}$ is covariantly conserved, $\nabla_\mu \tilde{T}^{\mu\nu} = 0$ which follows straightforward from diffeormorphism invariance because the Jordan frame metric couples very little to the matter stress tensor [2] i.e. covariant derivatives is used to preserve the physical laws invariant so that they are the same in all coordinate systems. The energy density for non-relativistic matter is defined as [1]

$$g^{\mu\nu}_{(i)} T^{(i)}_{\mu\nu} = -\tilde{\rho}_i. \tag{58}$$

So by considering a non-relativistic matter source to an FLRW ansatz for the metric [2]. Instead, its is more convenient to express $\tilde{\rho}_i$ with ρ_i so that $\rho_i = e^{\frac{3\beta_i\phi}{M_{Pl}}} \tilde{\rho}_i$, because it is conserved in the Einstein-frame [1] (for more information about the Einstein-frame can be found in Appendix [A.5]). Plugging all those things into equation (57) leads to

$$\nabla^2\phi = V^{'}(\phi) + \sum_i \frac{\beta_i}{M_{Pl}} \rho_i e^{\frac{\beta_i\phi}{M_{Pl}}}. \tag{59}$$

Taking the Taylor expansion over the exponential

$$e^{\frac{\beta\phi}{M_{Pl}}} = 1 + \frac{\beta\phi}{M_{Pl}} + \frac{1}{2!}\left(\frac{\beta\phi}{M_{Pl}}\right)^2 + ... \tag{60}$$

and only considering the zeroth order because of the weak field approximation $\beta\phi/M_{Pl} << 1$ [A.10] means that Poisson's equation can be rewritten as

$$\nabla^2\phi = V^{'}(\phi) + \sum_i \frac{\beta_i}{M_{Pl}}\rho_i. \tag{61}$$

When, considering that the matter fields couples in the same way:

$$\nabla^2\phi = V^{'}(\phi) + \frac{\beta}{M_{Pl}}\rho. \tag{62}$$

The right hand side of this expression shows that the dynamics of ϕ is not only directed by $V(\phi)$ but now also depends on ρ [1]. This is seen by considering a general scalar field Lagrangian and then using the Euler-Lagrangian equation to obtain the equation of motion.

1.8 The derivation of the ϕ-force

Here, the derivation of the ϕ -force also called the fifth force (induced by the scalar field ϕ) take place. The reason for using the conformal coupling in the geodesic equation here is because the conformal coupling $g^{(i)}_{\alpha\beta} = e^{2\beta_i\phi/M_{Pl}}g_{\alpha\beta}$ contains the interaction between the chameleon field and matter. The matter fields $\psi^{(i)}_m$ couple to each metric $g^{(i)}_{\alpha\beta}$ instead of $g_{\alpha\beta}$. Considering a free test particle with mass m of species i, a world line x^α which then only will experience gravity and the chameleon force have a geodesic which describe its straight path through the curved space-time:

$$\ddot{x}^\lambda + \tilde{\Gamma}^\lambda_{\alpha\beta}\dot{x}^\alpha\dot{x}^\beta = 0. \tag{63}$$

Which is the geodesic of $g^{(i)}_{\alpha\beta}$ instead of $g_{\alpha\beta}$. $\dot{x}^\alpha = \frac{dx^\alpha}{d\tilde{\tau}}$ and $\tilde{\tau}$ is the proper time while $\tilde{\Gamma}^\lambda_{\alpha\beta}$ is the Christoffel symbol defined as follow:

$$\tilde{\Gamma}^\lambda_{\alpha\beta} = \frac{1}{2}\tilde{g}^{\rho\lambda}(\partial_\alpha\tilde{g}_{\rho\beta} + \partial_\beta\tilde{g}_{\rho\alpha} - \partial_\rho\tilde{g}_{\alpha\beta}) \tag{64}$$

and the conformal transformation of the metric is:

$$\tilde{g}_{\alpha\beta} = e^{\frac{2\beta\phi}{M_{Pl}}}g_{\alpha\beta} \tag{65}$$

and the derivative with respect to ϕ and the metric $g_{\alpha\beta}$ gives [15]:

$$\partial_\rho \tilde{g}_{\alpha\beta} = (\frac{2\beta}{M_{Pl}}\partial_\rho\phi g_{\alpha\beta} + \partial_\rho g_{\alpha\beta})e^{\frac{2\beta\phi}{M_{Pl}}}. \tag{66}$$

Plug this back into equation (64):

$$\begin{aligned}\tilde{\Gamma}^\lambda_{\alpha\beta} &= \frac{1}{2}\big(\frac{2\beta}{M_{Pl}}g^{\rho\lambda}\partial_\alpha\phi g_{\rho\beta} + g^{\rho\lambda}\partial_\alpha g_{\rho\beta} + \frac{2\beta}{M_{Pl}}g^{\rho\lambda}\partial_\beta\phi g_{\rho\alpha} + g^{\rho\lambda}\partial_\alpha g_{\rho\alpha} \\ &\quad -\frac{2\beta}{M_{Pl}}g^{\rho\lambda}\partial_\rho\phi g_{\alpha\beta} - g^{\rho\lambda}\partial_\rho g_{\alpha\beta}\big). \end{aligned} \tag{66}$$

Using $\tilde{g}^{\rho\lambda} = e^{-2\beta/M_{Pl}}g^{\rho\lambda}$ and the inverse $\tilde{g}^{\rho\lambda} = e^{-2\beta/M_{Pl}}g^{\rho\lambda}$ so the exponentials has been canceled out in the expression above.

$$\begin{aligned}\tilde{\Gamma}^\lambda_{\alpha\beta} &= \frac{1}{2}\big(\frac{2\beta}{M_{Pl}}\big(g^{\rho\lambda}\partial_\alpha\phi g_{\rho\beta} + g^{\rho\lambda}\partial_\beta\phi g_{\rho\alpha} - g^{\rho\lambda}\partial_\rho\phi g_{\alpha\beta}\big) + g^{\rho\lambda}\partial_\alpha g_{\rho\beta} \\ &\quad +g^{\rho\lambda}\partial_\alpha g_{\rho\alpha} - g^{\rho\lambda}\partial_\rho g_{\alpha\beta}\big) \end{aligned} \tag{66}$$

Where $\Gamma^\lambda_{\alpha\beta} = 1/2(+g^{\rho\lambda}\partial_\alpha g_{\rho\beta} + g^{\rho\lambda}\partial_\alpha g_{\rho\alpha} - g^{\rho\lambda}\partial_\rho g_{\alpha\beta})$ and $g^{\rho\lambda}g_{\rho\beta} = \delta^\lambda_\beta$ finally gives

$$\tilde{\Gamma}^\lambda_{\alpha\beta} = \Gamma^\lambda_{\alpha\beta} + \frac{\beta}{M_{Pl}}(\partial_\alpha\phi\delta^\lambda_\beta + \partial_\beta\phi\delta^\lambda_\alpha - g^{\rho\lambda}\partial_\rho\phi g_{\alpha\beta}). \tag{67}$$

Plug everything back into the geodesic equation (63)

$$\ddot{x}^\lambda + \Gamma^\lambda_{\alpha\beta}\dot{x}^\alpha\dot{x}^\beta + \frac{\beta}{M_{Pl}}(2\partial_\alpha\phi\dot{x}^\alpha\dot{x}^\beta + g^{\rho\lambda}\partial_\rho\phi) = 0. \tag{68}$$

The third term in the geodesic equation contains a force-term while the second term represent the gravitational force. The first term inside the parentheses will vanish because the test particle with a mass m is in a static chameleon field i.e. $g^{00}\partial_0\phi$ (not time dependent) vanish so there will only be spatial terms left $g^{11}\partial_1\phi, g^{22}\partial_2\phi, g^{33}\partial_3\phi$. where $1 = x, 2 = y, 3 = z$.

$$\ddot{x}^\lambda + \Gamma^\lambda_{\alpha\beta}\dot{x}^\alpha\dot{x}^\beta + \frac{\beta}{M_{Pl}}g^{\rho\lambda}\partial_\rho\phi = 0 \tag{69}$$

$$\ddot{x}^\lambda + \Gamma^\lambda_{\alpha\beta}\dot{x}^\alpha\dot{x}^\beta = -\frac{\beta}{M_{Pl}}g^{\rho\lambda}\partial_\rho\phi \tag{70}$$

This means that the expression above can be rewritten with $\nabla = (\partial_x, \partial_y, \partial_z)$.

$$\ddot{x}^\lambda + \Gamma^\lambda_{\alpha\beta}\dot{x}^\alpha\dot{x}^\beta = -\frac{\beta}{M_{Pl}}g^{\rho\lambda}\nabla_\rho\phi \tag{71}$$

The expression on the LHS is the force and the force is defined $F = ma$ where a is the acceleration, it means that $\ddot{x} = a$ and it just means that the force has to be divided with the mass m here because the geodesic equation is not containing mass. Remembering that the metric g only is left with the spatial terms $g = (+, +, +)$. In a non-relativistic limit (equation (63)) a test particle in a static chameleon field ϕ with mass m will experience a chameleon force F_ϕ where ϕ is the potential to the chameleon force [15].

$$\frac{F_\phi}{m} = -\frac{\beta}{M_{Pl}}\nabla\phi. \tag{72}$$

1.9 The effective mass

Here we are consider a scenario where the scalar field creates a density dependent mass of the chameleon field [1.7]. One may realize that the effective potential plays a crucial role here, ρ exists in the effective potential and ϕ reacts on the value of ρ. It is basically about to balance the two contributions in the effective potential to get interesting effects from that, that means, to choose suitable forms on both the potential and the coupling so that the mass comes from the effective potential [2]. The potential of the chameleon scalar field can be generalized into an effective potential V_{eff} (see figure (2)):

$$V_{eff} = V(\phi) + \rho e^{\frac{\beta\phi}{M_{Pl}}}. \tag{73}$$

Even if $V(\phi)$ is monotonic, the effective potential can have a minimum as long as $\beta > 0$ [1]. $V(\phi)$ is decreasing and $V^{'}(\phi) < 0$ [2] is instead monotonically increasing [1]. Most of the contribution to the chameleon mass comes from the potential and that requires that $V^{''} > 0$ in order to remain stable [2].

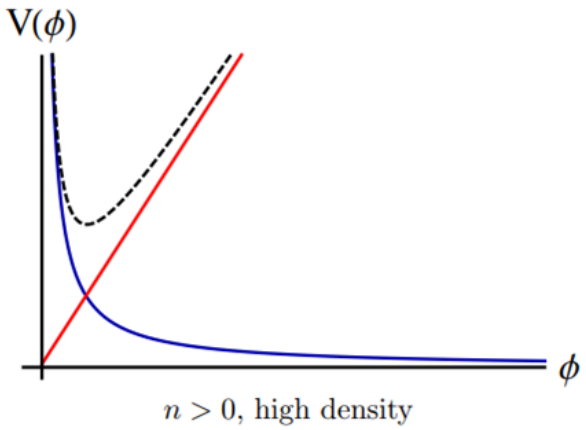

Figure 2: A plot of the chameleon potentials. The blue line respresents the self-interaction potential and the red is the matter coupling potential, while the the third dotted curve is the sum of both of them, i.e. the effective potential with a minimum [23]

The effective potential V_{eff} has its minimum when $\phi = \phi_{min}$:

$$V^{'}(\phi_{min}) + \frac{\beta}{M_{Pl}}\rho e^{\frac{\beta\phi_{min}}{M_{Pl}}} = 0 \tag{74}$$

[1]. The effective mass will be obtained by taking the second derivative of the effective potential

$$m^2_{eff}(\phi) = V^{''}_{eff}(\phi) = V^{''}(\phi) + \frac{\beta^2}{M^2_{Pl}}\rho e^{\frac{\beta\phi}{M_{Pl}}}. \tag{75}$$

The effective mass of the chameleon field is the mass of small fluctuations at ϕ_{min} [1]:

$$m^2_{min}(\phi_{min}) = V^{''}_{eff}(\phi_{min}) = V^{''}(\phi_{min}) + \frac{\beta^2}{M^2_{Pl}}\rho e^{\frac{\beta\phi_{min}}{M_{Pl}}}. \tag{76}$$

From these two equations above (74) and (75) it is seen that the field's minimum ϕ_{min} and its mass m_{min} are dependent on the local density and due to the conditions above and the fact that $V^{'}(\phi)$ is negative and monotonically increasing while $V^{''}(\phi)$ instead is positive and decreasing, results in small ϕ_{min} and large m_{min} (for larger values on ρ). This means that: the denser the local region is, the larger is the mass of the chameleon [1]. It is also necessary to have $V^{'''}(\phi) < 0$ so that m_{eff} really grows with ρ [2].

1.10 The thin shell model

The thin shell model is often used in the chameleon scalar theory [1]. As the name may suggest it is based on a model including a spherically symmetric massive compact object. Inside the massive objects core the chameleon field and its extra produced fifth force F_ϕ is completely suppressed due to the dense area inside the object. Assuming weak filed approximation results in a inner solution of the field profile which do not contribute. Instead a thin shell around the massive objects core will contribute to the outer solution of the field profile and there will be a fifth extra force F_ϕ. The analytic approach over the thin shell model and the outer solution of the field profile is presented in the Appendix [A.11]. In the next section 2, this will be treated in a different way, the procedure is based on a article by Terukina [4] and linked to the thin shell model through the weak field approximation [A.10].

2 Method

Here the procedure behind the resulting figures section (3) is presented and it is mainly based on a paper by Terukina [4] . The functions used here, the field profile $\phi(r)$ and the additional mass M_ϕ are plotted in Matlab and later presented with tables and figures in section [3].

2.1 The field profile $\phi(r)$

The field profile is density dependent and therefore the matter density $\rho(r)$ in the galaxy cluster is used in the field profile and it is defined by a Navarro-Frenk-White (NFW) profile [17]

$$\rho(r) = \frac{\rho_s}{r/r_s(1 + r/r_s)^2} \tag{77}$$

where ρ_s and r_s are characteristic parameters and good values for those can be estimated by using that the virial mass within a virial radius r_{vir} of the cluster is $M_{vir} \simeq 10^{14} M_{sol}$ ($M_{sol} = 1.989 \times 10^{30}$ kg) and a concentration parameter $c = r_{vir}/r_s = 5$. For a cold Dark Matter scenario, the overdensity contrast is $\Delta_c \approx 100$ which is used in the equation (79) below and it comes from a spherical collapse model. ρ_c is the critical density and $\Delta_c \rho_c$ is the average density which defines r_{vir}. The characteristic radius of a galaxy cluster is:

$$r_s = \frac{1}{c}\left(\frac{M_{vir}}{(4\pi/3)\Delta_c \rho_c}\right)^{1/3} \tag{78}$$

and the characteristic density is then:

$$\rho_s = \frac{M_{vir}}{4\pi r_s^3}\left(\log(1+c) - \frac{c}{1+c}\right)^{-1}. \tag{79}$$

Now the matter density is put into the Poisson equation (62) obtained earlier in section [1.7]:

$$\nabla^2\phi = V^{'}(\phi) + \frac{\beta}{M_{Pl}}\rho(r) = V^{'}(\phi) + \frac{\beta}{M_{Pl}}\frac{\rho_s}{r/r_s(1+r/r_s)^2} \tag{80}$$

and from this we get the field profile for both the inner and the outer region of the galaxy cluster. Lets first look at the inner solution by putting $\nabla^2\phi = 0$

$$V^{'}(\phi) + \frac{\beta}{M_{Pl}}\rho = 0 \tag{81}$$

$$\frac{dV(\phi)}{d\phi} = -\frac{\beta}{M_{Pl}}\rho \tag{82}$$

and now by using the power-law potential $V = \frac{\Lambda^{n+4}}{\phi^n}$ where the derivative of that is $\frac{dV(\phi)}{d\phi} = \frac{n\Lambda^{n+4}}{\phi^{n+1}}$. Put it back into the expression above and it results in:

$$\frac{n\Lambda^{n+4}}{\phi^{n+1}} = -\frac{\beta}{M_{Pl}}\rho \tag{83}$$

$$\phi^{n+1} = -\frac{nM_{Pl}\Lambda^{n+4}}{\rho\beta} \tag{84}$$

This is an expression for ϕ. The characteristic ϕ_s can then be defined as:

$$\phi_s^{n+1} = -\frac{nM_{Pl}\Lambda^{n+4}}{\rho_s\beta} \tag{85}$$

is characteristic for each galaxy cluster in concern. While the field profile far outside the galaxy cluster is:

$$\phi_\infty^{n+1} = -\frac{nM_{Pl}\Lambda^{n+4}}{\rho_\infty\beta} \tag{86}$$

Putting in the expression for the matter density $\rho(r)$ i.e. put equation (77) into equation (87):

$$\phi^{n+1} = \frac{\frac{r}{r_s}(1+r/r_s)^2 nM_{Pl}\Lambda^{n+4}}{\rho_s\beta} = \frac{r}{r_s}(1+r/r_s)^2\phi_s^{n+1}. \tag{87}$$

This is the expression for the inner solution when the radius r is less than the critical radius R_o. R_o is a transition scale used as a condition to make the transition between the inner and the outer solution is smoothly consistent and it is governed by β and ϕ_∞. R_o will be used in the boundary conditions later. The inner solution represents the region where the chameleon suppressing the scalar field and the chameleon field does not mediate a fifth force. The outer solution is instead obtain by putting $V^{'}(\phi) = 0$, $r > R_o$ and integrating this equation two times:

$$\nabla^2\phi = \frac{\beta}{M_{Pl}}\rho(r) \tag{88}$$

Re-write $\nabla^2\phi$ in spherical coordinates (only considering r) and plug in the expression for $\rho(r)$

$$\frac{1}{r^2}\frac{\partial}{\partial r}\big(r^2\frac{\partial\phi}{\partial r}\big) = \frac{\beta\rho_s}{r/r_s(1+r/r_s)^2M_{Pl}} \tag{89}$$

$$\frac{\partial}{\partial r}\big(r^2\frac{\partial\phi}{\partial r}\big) = \frac{\beta\rho_s r_s r}{(1+r/r_s)^2M_{Pl}} \tag{90}$$

Now integrating one time with respect to r and divide the RHS with r^2

$$\frac{\partial\phi}{\partial r} = \frac{\beta\rho_s r_s^3}{r^2M_{Pl}}\left(\frac{1}{1+r/r_s} + \log\left(r/r_s+1\right)\right) + \frac{C}{r^2}. \tag{91}$$

Where C is an integration constant. Solving out $\phi(r)$ gives

$$\phi(r) = \frac{\beta\rho_s r_s^3}{M_{Pl}}\int \mathrm{d}r\frac{1}{r^2}\frac{1}{1+r/r_s} + \frac{\beta\rho_s r_s^3}{M_{Pl}}\int(\frac{1}{r^2}\log\left(r/r_s+1\right)\Big) + \frac{C}{r^2})\mathrm{d}r. \tag{92}$$

Lets integrate the first term with respect to r results in:

$$\int \mathrm{d}r\frac{1}{r^2}\frac{1}{1+r/r_s} \tag{93}$$

$$= \quad -\frac{1}{r} + \frac{1}{r_s}\log\left(1/r_s+1/r\right) \tag{93}$$

Integrating the second term is a little bit more complicated so lets do a partial integration first:

$$\int \frac{1}{x^2}\log\left(ax+b\right)dx = -\frac{1}{x}\log\left(ax+b\right) + \int\frac{1}{x}\frac{1}{ax+b}a \tag{94}$$

$$= -\frac{1}{x}\log(ax+b) - \frac{a}{b}\log\left(\frac{ax+b}{x}\right) \tag{95}$$

$a = 1/r_s$, $b = 1$ and $x = r$ and plug it in the second term [**?**]:

$$= -\frac{\log(r/r_s+1)}{r} - \frac{1}{r_s}\log\left(\frac{r/r_s+1}{r}\right). \tag{96}$$

Finally, the third term as well. Now, plug all the three integrated terms back into $\phi(r)$ in equation (92):

$$\phi(r) = \frac{\beta\rho_s r_s^2}{M_{Pl}}\left(\frac{1}{r_s}\log(1/r_s+1/r_s) - \frac{1}{r}\log(r/r_s+1) - \frac{1}{r_s}\log(1/r_s+1/r)\right) - \frac{C}{r} + \phi_\infty. \tag{95}$$

ϕ_∞ is the second integration constant but it is very important because it determines the effectivity of the screening mechanism, describing the chameleon field far away from the galaxy cluster

$$\phi_\infty = -\left(\frac{nM_{Pl}\Lambda^{n+4}}{\rho_\infty\beta}\right)^{1/n+1}. \tag{96}$$

ρ_∞ is the background density which will later be varied in the plots in section [3] for $\rho_\infty = 0.1 \times 0.3\rho_c$, $0.5 \times 0.3\rho_c$, $0.3\rho_c$, $0.6\rho_c$ and ρ_c where the critical density is $\rho_c = 3H_0^2 M_{Pl}^2$ and H_0 is the Hubble parameter

$$\phi_{out} = -\frac{\beta\rho_s r_s^3}{M_{Pl}}\frac{\log(1+r/r_s)}{r} - \frac{C}{r} + \phi_\infty. \tag{97}$$

Following boundary condition is used in order to solve out C and ϕ_∞ when $r = r_c$:

$$\phi_{int}(r_c) = \phi_{out}(r_c) \tag{98}$$

$$\phi'_{int}(r_c) = \phi'_{out}(r_c). \tag{99}$$

After putting these two solution equal to each other (as above) and after some calculations, the result is:

$$\frac{R_o}{r_s}(1+R_o/r_s)^2\phi_s^{n+1} = -\frac{\beta\rho_s r_s^3}{M_{Pl}}\frac{\log(1+R_o/r_s)}{R_o} - \frac{C}{R_o/r_s} + \phi_\infty \tag{100}$$

and finally solving out the integration constant C as well as the critical radius R_o:

$$C = -\frac{\beta \rho_s r_s^2}{M_{Pl}} \log\left(1 + R_o/r_s\right) + \phi_\infty R_o/r_s \tag{101}$$

as well as the integration constant ϕ_∞

$$\phi_\infty - \frac{\beta \rho_s r_s^2}{M_{Pl}} (1 + R_o/r_s)^{-1} \simeq 0. \tag{102}$$

Solving out r_c from this last equation gives:

$$R_o = \frac{\beta \rho_s r_s^3}{M_{Pl} \phi_\infty} - r_s \tag{103}$$

which is the critical radius, also known as the transition scale between the inner and the outer solution of the galaxy cluster's field profile.

The characteristic density ρ_s inside the galaxy cluster is $\rho_s \gg \rho_\infty$ because it is a dense region and the chameleon field get suppressed which in turns means that $\phi_s \ll \phi_\infty$. This is the reason why the interior solution of the field profile is $\phi_{int} \simeq 0$ and by that the characteristic solution will also be $\phi_s \simeq 0$.

Those transition relations do not depend on the chameleon parameters of the scalar fields potential Λ and n where ϕ_∞ is considered as a DOF of the model which in turn depends on the environment of the cluster. So, ϕ_∞ is the chameleon field far out at its minimum of the effective potential.

2.2 The hydrostatic mass

In this section the hydrostatical mass which contains the thermal and non-thermal mass of the galaxy clusters gas components will be considered, it is also is considered in this article [4]. Considering a spherically symmetric system of gas and dark matter. Where both are baryonic and the dark matter are coupling to the chameleon field and they both experience the Newtonian gravitational force as well as the chameleon force F_ϕ.

The mass equation for a dark matter halo within a radius r is:

$$M(< r) = 4\pi \int_0^r dr r^2 \rho(r) \tag{104}$$

where ρ is the matter density in the galaxy cluster from a NFW profile in

equation (77). Plug in equation (77) and integrate over r:

$$\begin{aligned} M(<r) &= 4\pi \int_0^r dr r^2 \frac{\rho_s}{r/r_s(1+r/r_s)^2} \\ &= 4\pi\rho_s r_s \int_0^r dr \frac{r}{(1+r/r_s)^2} \\ &= 4\pi\rho_s r_s^3 \left(\frac{1}{1+r/r_s} + \log(r/r_s+1) - 1 - \log 1 \right) \\ &= 4\pi\rho_s r_s^3 \left(\frac{1-1-r/r_s}{1+r/r_s} + \log(r/r_s+1) \right) \\ &= 4\pi\rho_s r_s^3 \left(\log(r/r_s+1) - \frac{r/r_s}{1+r/r_s} \right) \end{aligned} \tag{101}$$

This mass will later referred to a total mass of the system and it is often used as the weak lensing mass M_{WL}. The virial mass M_{vir} of a halo within the radius r_{vir}:

$$M_{vir} = \frac{4\pi}{3} r_{vir}^3 \Delta_c \rho_c \tag{102}$$

where $\Delta_c\rho_c$ is the average density (see section [2]).

2.3 The additional mass M_ϕ

In this thesis the focus will also be laid on the additional mass M_ϕ (see section [2.2]) which will be plotted for different values of Λ, β and ρ_∞ in section [3]. This is done in order to compare with the virial mass M_{vir} in section [3].

As in the previous section [2.3], consider a spherically symmetric system containing dark matter and gas, like a galaxy cluster in hydrostatic equilibrium. The equation for the gas component can be written as

$$\frac{1}{\rho_{gas}(r)} \frac{\mathrm{d}P_{total}}{\mathrm{d}r} = -\frac{GM_{GR}(<r)}{r^2}. \tag{103}$$

This equation is given for the general relativity (GR) case without the scalar field ϕ and the hydrostatical mass $M_{GR} = M_{thermal} + M_{non-thermal}$. The additional part containing the force $F_\phi = -\frac{\beta}{M_{Pl}} \frac{\mathrm{d}\phi}{\mathrm{d}r}$ is added:

$$\frac{1}{\rho_{gas}(r)} \frac{\mathrm{d}P_{total}}{\mathrm{d}r} = -\frac{GM_{GR}(<r)}{r^2} - \frac{\beta}{M_{Pl}} \frac{\mathrm{d}\phi}{\mathrm{d}r}. \tag{104}$$

While the hydrostatic equilibrium equation is:

$$\frac{1}{\rho(r)}_{gas}\frac{\mathrm{d}P_{total}}{\mathrm{d}r} = -\frac{GM(<r)}{r^2} \tag{105}$$

The chameleon force modifies the extra mass inferred from the hydrostatic equilibrium like $M(<r) = M_{GR}(<r) + M_\phi$. From this it can be concluded that:

$$\frac{GM_\phi(<r)}{r^2} = -\frac{\beta}{M_{Pl}}\frac{\mathrm{d}\phi}{\mathrm{d}r} \tag{106}$$

and the extra mass is then [4]:

$$M_\phi = -\frac{r^2}{G}\frac{\beta}{M_{Pl}}\frac{\mathrm{d}\phi}{\mathrm{d}r}. \tag{107}$$

In presence of a chameleon field the extra force F_ϕ is added to the RHS of equation (103) and the hydrostatic equilibrium gets modified see section [1.9]. F_ϕ modifies the hydrostatic equilibrium mass M when the extra mass M_ϕ is added to its equation. In the paper by Terukina [4] they define the hydrostatical mass as:

$$M(<r) = M_{thermal} + M_{non-thermal} + M_\phi. \tag{108}$$

Where

$$M_{thermal}(r) \equiv -\frac{r^2}{G\rho_{gas}(r)}\frac{dP_{thermal}(r)}{dr} \tag{109}$$

$$M_{non-thermal}(r) \equiv -\frac{r^2}{G\rho_{gas}(r)}\frac{dP_{non-thermal}(r)}{dr} \tag{110}$$

and the parameters are obtained from different kind of observations, X-ray temperature and X-ray surface brightness [4]. Later they integrate over the NFW density profile in equation (138) in order to get the weak lensing mass M_{WL} :

$$M_{WL} = 4\pi\rho_s r_s^3\left(\log(1+r/r_s) - \frac{r/r_s}{1+r/r_s}\right). \tag{111}$$

This is the integral used for integrating the mass of a dark matter halo within a radius r in equation (138) used earlier in section [2.2]. In the paper [4] they compare the hydrostatical with the weak lensing mass, first without

the modification from the additional mass i.e. only considering effects from Newtonian gravitational force and then with the additional mass to look at the dispersion between the results. This means by looking at equation (138) and equation (108) and assuming hydrostatical equilibrium, the weak lensing mass, M_{WL} is:

$$M_{WL} = M_{thermal} + M_{non-thermal} + M_{\phi}. \tag{112}$$

The reconstructed hydrostatic mass with observational data is reduced in the presence of the force from the chameleon field F_ϕ which creates an attractive force, i.e. when the additional mass M_ϕ is added. How much it is contributing depends on different values of β and ρ_∞ and it is presented in section [3]. This phenomenon appears especially for higher values of β and only in regions beyond the critical radius R_o. This creates a condition that the critical radius has to be less than the radius of the cluster $R_o < r_{cluster}$ which puts an upper bound on $\beta M_{Pl}/\phi_\infty$.

3 Results

In this section the resulting plots over the field profile $\phi(r)$ and the additional mass M_ϕ/M_{vir} are presented for different values of the self interacting constant Λ, the coupling strength β and the background density ρ_0 as well for the background density ρ_∞ far away from the galaxy cluster. The value on β was varied by first letting $\beta = 1/\sqrt{6}$ for all the four different values of the density $\rho_0 = 0.3\rho_c$, $\rho_0 = 0.6\rho_c$ and when $\rho_0 = \rho_c$ as well as for $\rho_\infty = 0.1 \times 0.3\rho_c$ and later do the same runs for the value of $\beta = 1$. At this stage,there are indications that a stronger coupling to the matter fields (remembering that in this case β is coupling to both the baryonic as well as the dark matter fields), results in a longer range for the critical radius R_o where the transition from the inner to the outer regions of the galaxy cluster occurs which was presented in section [2]. This slightly affects the value of the field profile far outside from the galaxy cluster which will be noticed in the Tables for each value of Λ. In general, R_o got a value which was larger than the considered range of r. When r was plotted between 0 to 10000 kpc for $\Lambda = 4.66$ eV (Table 1) and $\Lambda = 10$ eV (Table 2), $\phi(r)$ did not contribute over the considered range for all values of ρ_∞ and β. This is due to the fact, that there will only be a contribution from the field profile outside the galaxy cluster which appears after the transition scale i.e when the critical radius is within the range of r. The field profile was plotted with respect to r over different ranges depending on the value of Λ, generally speaking, larger values on Λ gave smaller R_o and by that, also smaller range on r. This pattern can be

seen both on the values over R_o and r throughout all of the tables and the figures presented in section [3.1] - [3.3]. As mentioned in section [2] the virial mass is $M_{vir} \sim 10^{14} M_{sol}$ and the virial radius is $r_{vir} = 1215$ kpc which are typical observational values. The values of $\phi(r)$ and M_ϕ/M_{vir}, in the tables are taken at the last point for the range of r i.e. if r is ranging over 0 to 10000 kpc (like in Table 1), the value on $\phi(r)/M_{Pl}$ and M_ϕ/M_{vir} in Table 1 is taken at the point when $r = 10000$ kpc.

3.1 When $\Lambda = 4.66$ eV

We look at $\Lambda = 4.66$ eV and consider r to be running from 0 to 10000 kpc. Beyond the value of $r = 10000$ kpc, the contribution from another galaxy most likely starts to contribute as well. In average the distance to the next galaxy cluster is about 20000 kpc. The value on Λ is taken from this paper by Pourhasan [19].

ρ_∞	β	$\frac{\phi_\infty}{M_{Pl}}$	R_o (kpc)	$\frac{\phi(r)}{M_{Pl}}$	$\frac{\phi(r_{vir})}{M_{Pl}}$	$\frac{M_\phi(r)}{M_{vir}}$	$\frac{M_\phi(r_{vir})}{M_{vir}}$
$0.03\rho_c$	$1/\sqrt{6}$	1.38×10^{-6}	2723	4.97×10^{-7}	-	-0.41	-
$0.03\rho_c$	1	8.82×10^{-7}	11129	-	-	-	-
$0.15\rho_c$	$1/\sqrt{6}$	6.17×10^{-7}	6390	4.92×10^{-8}	-	-0.146	-
$0.15\rho_c$	1	3.95×10^{-7}	25186	-	-	-	-
$0.3\rho_c$	$1/\sqrt{6}$	4.37×10^{-7}	9137	1.63×10^{-9}	-	-0.03	-
$0.3\rho_c$	1	2.79×10^{-7}	35719	-	-	-	-
$0.6\rho_c$	$1/\sqrt{6}$	3.07×10^{-7}	13024	-	-	-	-
$0.6\rho_c$	1	1.97×10^{-7}	50614	-	-	-	-
ρ_c	$1/\sqrt{6}$	2.39×10^{-7}	16883	-	-	-	-
ρ_c	1	1.53×10^{-7}	65414	-	-	-	-

Table 1: When $\Lambda = 4.66$ eV for diffrent values on the background density ρ_∞ far away from the galaxy cluster. The values of $\phi(r)/M_{Pl}$ and $M_\phi(r)/M_{vir}$ in the Table are taken at the last point of the range of r, i.e. in this case for $r = 10000$ kpc. For larger values of ρ_∞, i.e. the environment is denser, gives slightly smaller values of ϕ_∞ but the critical radius R_o is large in both scenarios. In fact, R_o is too large ($r < R_o$) and only leads to a contribution for $\phi(r)/M_{Pl}$ and M_ϕ/M_{vir} when $\rho_\infty = 0.1 \times 0.3\rho_c$, $0.5 \times 0.3\rho_c$ and when $0.3\rho_c$ for $\beta = 1/\sqrt{6}$. There is no contribution at the virial radius $r_{vir} = 1215$ kpc because $r_{vir} < R_o$. Notice that the value on M_ϕ is negative! The reason for that is that the fifth force F_ϕ is attractive (see section [2.3]). There is no contribution from the functions at r_{vir} because $R_o > r_{vir}$

In Table 1, it is clear that R_o reaches out over a large range for higher values of β i.e. the coupling strength is stronger and coupling harder to the matter fields which also can be seen with increased background density. In Figure 3 this can be seen on the functions $\phi(r)/M_{Pl}$ in Figure 3 and M_ϕ/M_{vir} in Figure 4 which are assumed to be zero before the critical radius R_o. The functions start to increase after their particular value of R_o (see Table 1) and due to that there are only contributions from the case for $\rho_\infty = 0.1 \times 0.3\rho_c$, $0.5 \times 0.3\rho_c$ and $0.3\rho_c$ when $\beta = 1/\sqrt{6}$ with r ranging from 0 to 10000 kpc. Notice that in Table 1 when β is increasing, ϕ_∞ is decreasing but the critical radius R_o is rapidly growing. $\phi(r)$ is also growing for larger values of β.

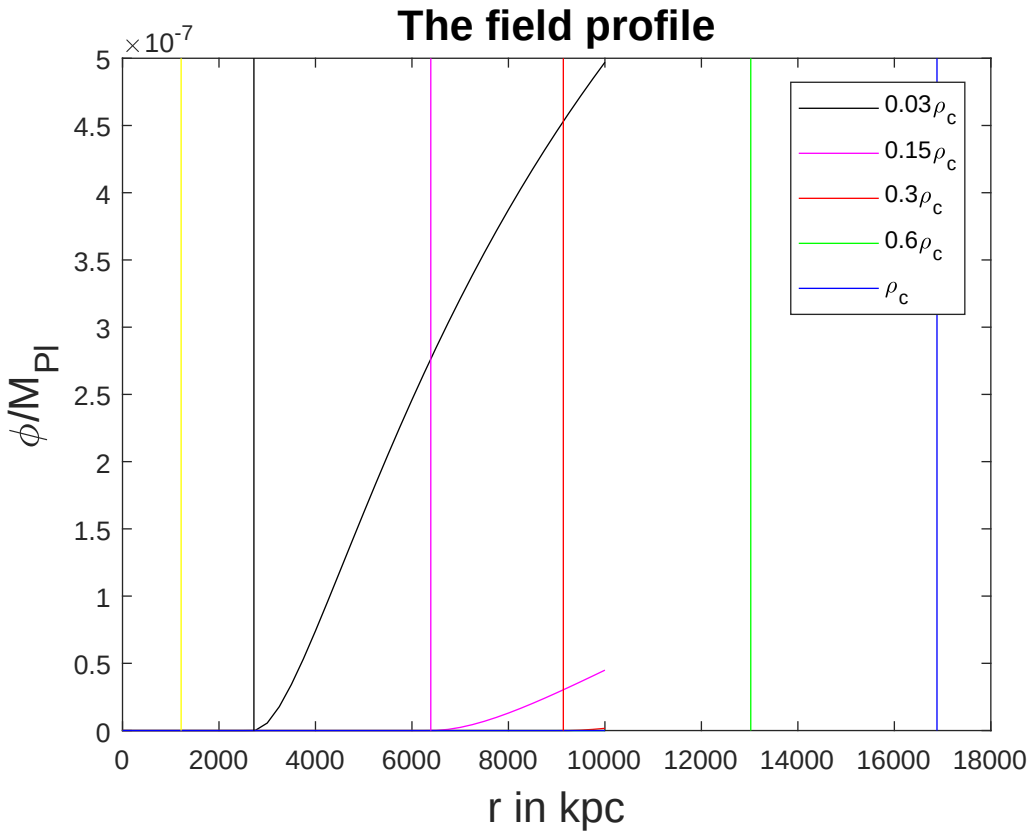

Figure 3: A plot over $\phi(r)/M_{Pl}$ with respect to r ranging from 0 to 10000 kpc for $\Lambda = 4.66$ eV and $\beta = 1/\sqrt{6}$. The grey curve is when $\rho_\infty = 0.1 \times 0.3\rho_c$ with a grey vertical line marking out the critical radius R_o for that particular function. The magenta coloured curve is for $\rho_\infty = 0.5 \times 0.3\rho_c$ with a magenta coloured vertical line for its R_o. $\phi(r)/M_{Pl}$ is zero before R_o. After R_o, $\phi(r)/M_{Pl}$ is starting to increase. The other values of $\phi(r)/M_{Pl}$ for ρ_∞ are zero except from the red tiny line seen as a dot on the right side of the r-axis, represents the case when $\rho_\infty = 0.3\rho_c$ with its R_o at 9137 kpc (red vertical line marking out its R_o) and this is because the critical radius R_o is too large (Table 1). The virial radius is marked with a yellow vertical line r_{vir} is at 1215 kpc.

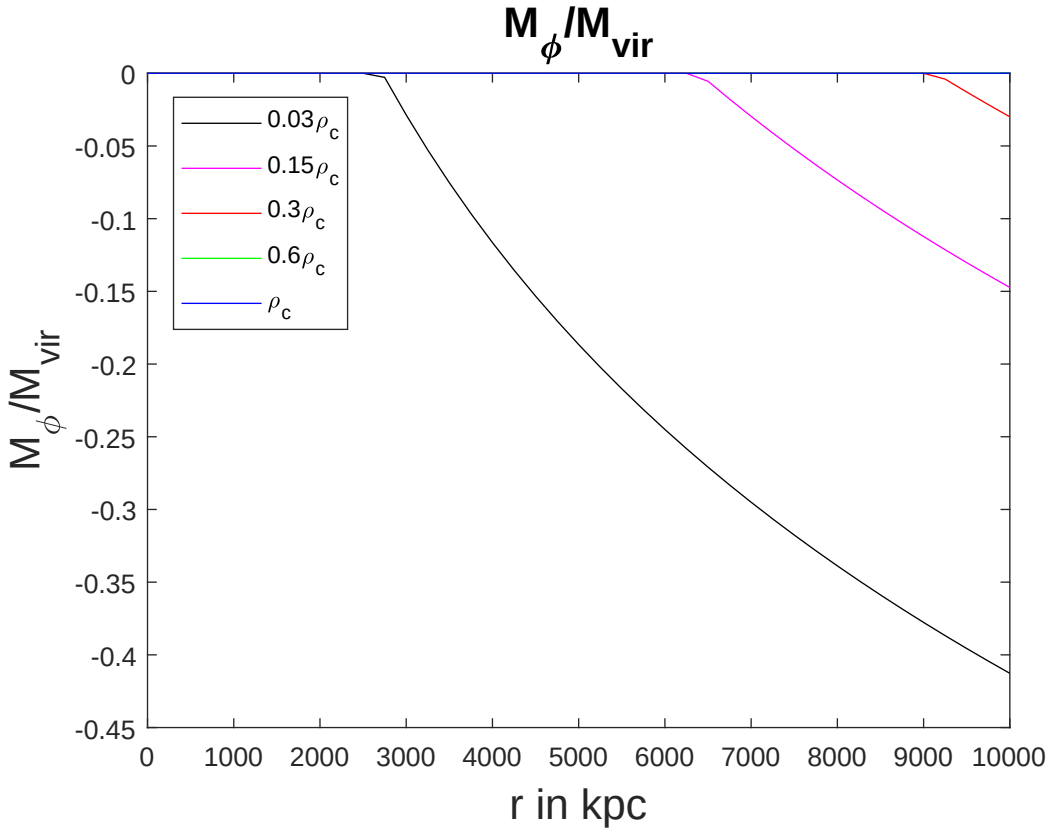

Figure 4: A plot over M_ϕ/M_{vir} with respect to r ranging from 0 to 10000 kpc when $\Lambda = 4.66$ eV and $\beta = 1/\sqrt{6}$. The grey curve is when $\rho_\infty = 0.1 \times 0.3\rho_c$, a magenta coloured curve representing when $\rho_\infty = 0.5 \times 0.3\rho_c$ and the red curve (seen in the right upper corner of the figure) is when $\rho_\infty = 0.3\rho_c$ with R_o at 9137 kpc while the two other curves do not appear here because the value for R_o is too large ($r < R_o$). Each value of R_o can be found in Table 1. The same tendency as for the function $\phi(r)/M_{Pl}$ can be seen here, M_ϕ is zero until it reaches R_o and then starts to decrease. The reason why M_ϕ has a negative value is because the fifth force F_ϕ is attractive, this is explained further in section [2.3].The virial radius has a yellow vertical line marking out r_{vir} is at 1215 kpc.

3.2 When $\Lambda = 10$ eV

Here we are looking at $\Lambda = 10$ eV with r ranging from 0 to 10000 kpc.

ρ_∞	β	$\frac{\phi_\infty}{M_{Pl}}$	R_o (kpc)	$\frac{\phi(r)}{M_{Pl}}$	$\frac{\phi(r_{vir})}{M_{Pl}}$	$\frac{M_\phi(r)}{M_{vir}}$	$\frac{M_\phi(vir)}{M_{vir}}$
$0.03\rho_c$	$1/\sqrt{6}$	9.31×10^{-6}	197	7.84×10^{-6}	3.73×10^{-6}	-0.91	-0.28
$0.03\rho_c$	1	5.95×10^{-6}	1443	3.28×10^{-6}	-	-3.52	-
$0.15\rho_c$	$1/\sqrt{6}$	4.17×10^{-6}	741	2.90×10^{-6}	2.86×10^{-7}	-0.74	-0.11
$0.15\rho_c$	1	2.66×10^{-6}	3527	3.28×10^{-6}	-	-2.0	-
$0.3\rho_c$	$1/\sqrt{6}$	2.95×10^{-6}	1148	1.79×10^{-6}	2.33×10^{-9}	-0.64	-0.01
$0.3\rho_c$	1	1.88×10^{-6}	5088	5.41×10^{-7}	-	-1.33	-
$0.6\rho_c$	$1/\sqrt{6}$	2.08×10^{-6}	1724	1.05×10^{-6}	-	-0.54	-
$0.6\rho_c$	1	1.33×10^{-6}	7296	2.13×10^{-7}	-	-0.62	-
ρ_c	$1/\sqrt{6}$	1.61×10^{-6}	2296	6.7×10^{-7}	-	-0.46	-
ρ_c	1	1.03×10^{-6}	9490	7.86×10^{-8}	-	-0.10	-

Table 2: For $\Lambda = 10$ eV. The values of $\phi(r)/M_{Pl}$ in this table are taken at the last point for the range of r i.e. in this case when $r = 10000$ kpc for the background density ρ_∞. Here $\phi(r)/M_{Pl}$ and M_ϕ/M_{vir} contributes (the functions starts to increase) after R_o ends because $R_o < r$. Also, M_ϕ gets larger than the virial mass M_{vir} for the case when ρ_∞ has a low value and the coupling is strong ($\beta = 1$) which does not make sense but it is coupling harder to matter which creates this scenario of a heavier contribution from the additional mass. See section [2.3] for explanation for the negative value on M_ϕ.

The same pattern as in the previous section [3.1] is noticeable here in Table 2. It is once again for sure that the surrounding density ρ_∞ does not have the same impact on the field profile $\phi(r)$ as the coupling strength β has, see figures 5 and 6 except for very low values of ρ_∞. A larger value on Λ also results in higher values of the additional mass M_ϕ (figure 7), especially for values when $\beta = 1$ in Figure 8. M_ϕ is decreasing with increased density ρ_∞ as can be seen by comparing the two figures, Figures 7 and Figure 8.

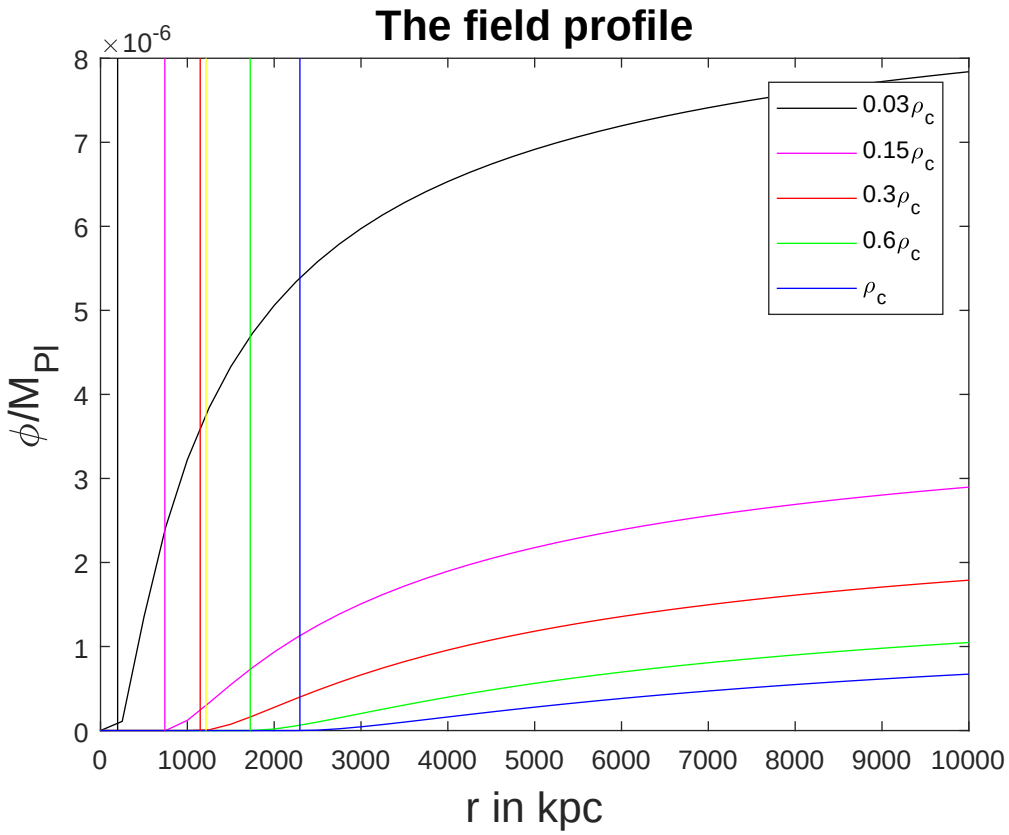

Figure 5: A plot over $\phi(r)/M_{Pl}$ with respect to r ranging from 0 to 10000 kpc for $\Lambda = 10$ eV and $\beta = 1/\sqrt{6}$. The grey curve is for $\rho_\infty = 0.1 \times 0.3\rho_c$ and it shows that $\phi(r)/M_{Pl}$ grows rapidly in the beginning i.e. until R_o (Table 2) and the same behavior can be observed for the rest of the curves except that their increasing rate is less than for ρ_∞ (Table 2). The magenta coloured curve is for $\rho_\infty = 0.5 \times 0.3\rho_c$ with a vertical line in magenta, marking out where its R_o is situated on the axis.The red curve is when $\rho_\infty = 0.3\rho_c$ with a red vertical line for R_o, the green curve is for $\rho_0 = 0.6\rho_c$ with a green vertical line for its R_o and the blue one is when $\rho_0 = \rho_c$ with a blue vertical line for its R_o. $r_{vir} = 1215$ kpc with a yellow vertical line.

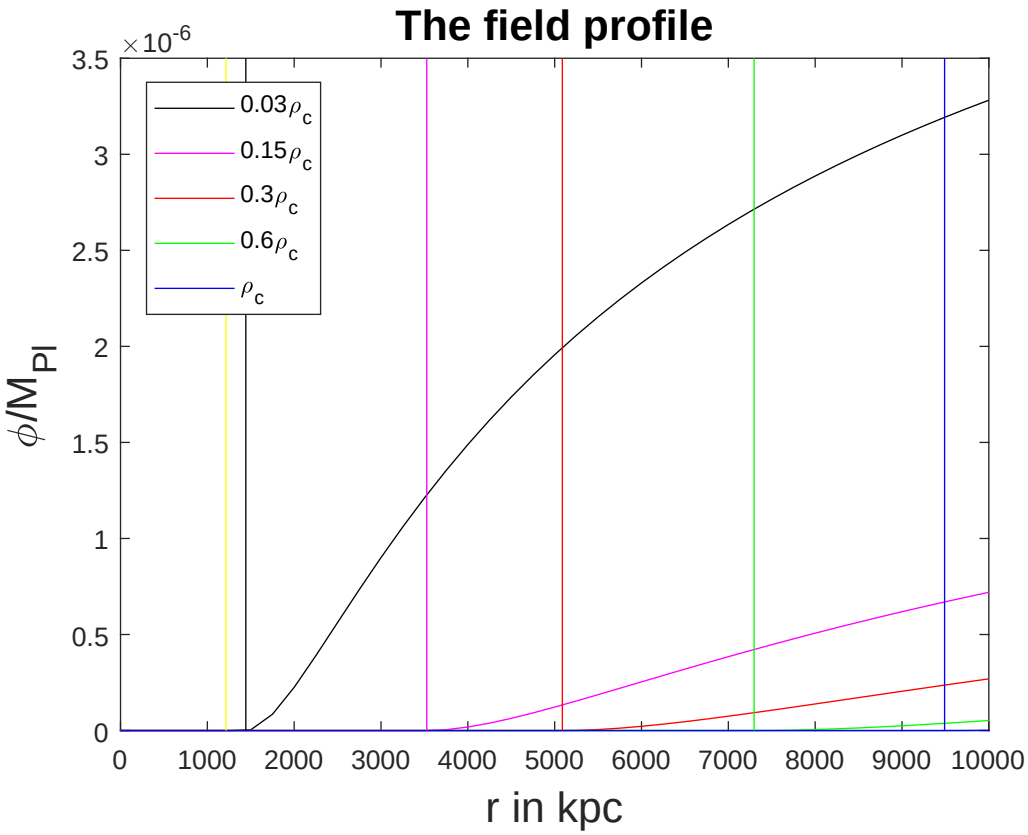

Figure 6: A plot over $\phi(r)/M_{Pl}$ with respect to r ranging from 0 to 10000 kpc for $\Lambda = 10$ eV and $\beta = 1$. The grey curve is for $\rho_\infty = 0.1 \times 0.3\rho_c$ with a grey vertical line for its R_o. The magenta coloured curve for $\rho_\infty = 0.5 \times 0.3\rho_c$ with a vertical line in magenta, marking out where its R_o are situated on the axis. The red curve is when $\rho_\infty = 0.3\rho_c$ also with a vertical line (red) marking out R_o in that case and the green curve is for $\rho_\infty = 0.6\rho_c$ with a green vertical line for R_o while the blue one is when $\rho_\infty = \rho_c$ (with a blue vertical line for R_o) which only can been seen as a blue straight line on the x-axis due to that $\phi(r)/M_{Pl}$ is zero almost the whole way on the x-axis because $R_o = 9490$ kpc. $r_{vir} = 1215$ kpc has a yellow vertical line.

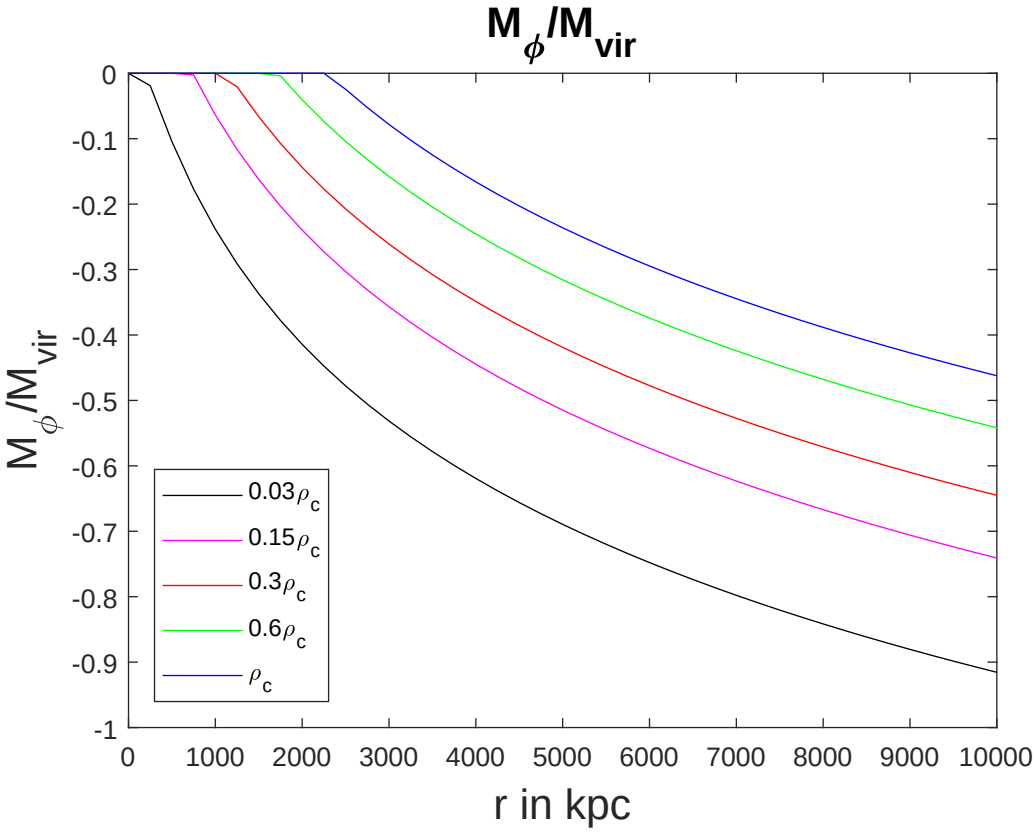

Figure 7: A plot over M_ϕ/M_{vir} with respect to r ranging from 0 to 10000 kpc for $\Lambda = 10$ eV and $\beta = 1/\sqrt{6}$. The grey curve is for when $\rho_\infty = 0.1 \times 0.3\rho_c$,the magenta coloured curve for $\rho_\infty = 0.5 \times 0.3\rho_c$, the red curve is when $\rho_\infty = 0.3\rho_c$, the green curve is for $\rho_\infty = 0.6\rho_c$ and the blue one is when $\rho_\infty = \rho_c$. They all have their starting point at their particular value of R_o which can be found in Table 2. r_{vir} is at 1215 kpc. See section [2.3] for more information about the negative value on M_ϕ.

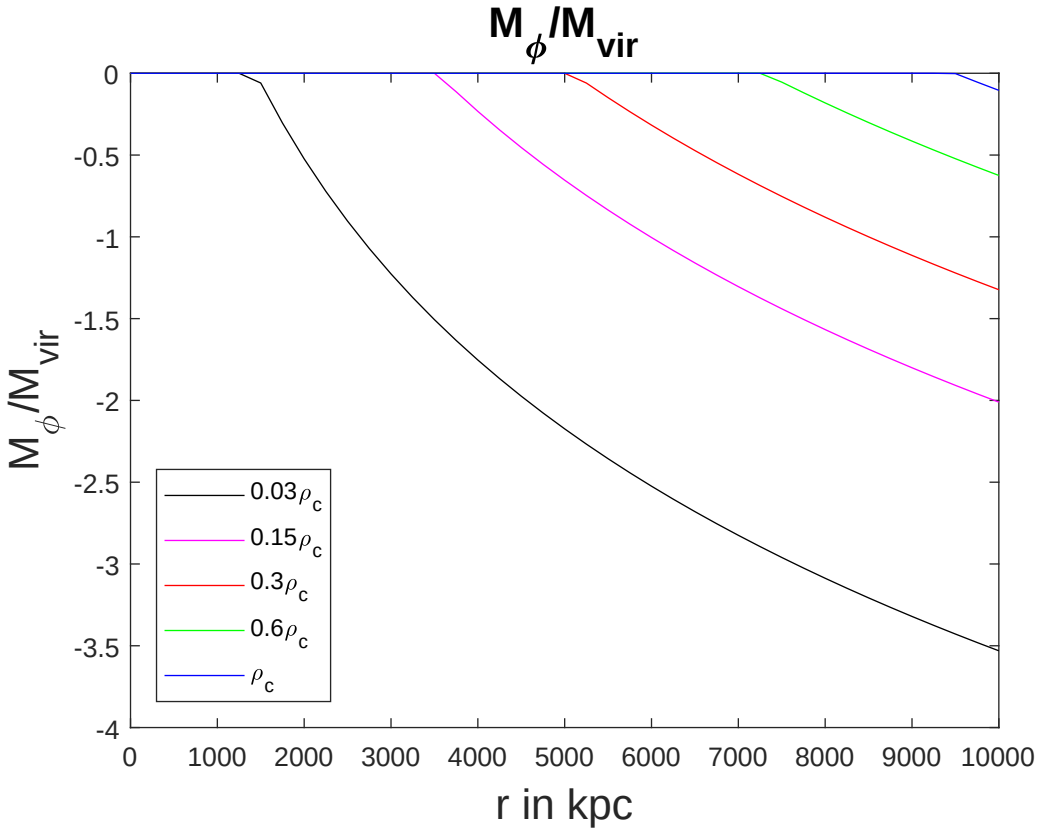

Figure 8: A plot over M_ϕ/M_{vir} with respect to r ranging from 0 to 10000 kpc for $\Lambda = 10$ eV and $\beta = 1$. The grey curve is for when $\rho_\infty = 0.1 \times 0.3\rho_c$ where the value of $R_o = 1148$ kpc.The magenta coloured curve for $\rho_\infty = 0.5 \times 0.3\rho_c$, the red curve is when $\rho_\infty = 0.3\rho_c$ with $R_o = 5088$ kpc, the green curve is for $\rho_\infty = 0.6\rho_c$ with $R_o = 7296$ kpc and the blue one is when $\rho_\infty = \rho_c$ for $R_o = 9490$ kpc. $r_{vir} = 1215$ kpc. See section [2.3] for more information about the negative value of M_ϕ.

3.3 When $\Lambda = 16.8$ eV

Looking at $\lambda = 16.8$ eV with r considered to be running from 0 to 5000 kpc.

ρ_∞	β	$\frac{\phi_\infty(r)}{M_{Pl}}$	R_o (kpc)	$\frac{\phi(r}{M_{Pl}}$	$\frac{\phi(r_{vir})}{M_{Pl}}$	$\frac{M_\phi(r)}{M_{vir}}$	$\frac{M_\phi(r_{vir})}{/M_{vir}}$
$0.03\rho_c$	$1/\sqrt{6}$	3.41×10^{-5}	-122	3.16×10^{-5}	3.41×10^{-5}	-0.74	-0.33
$0.03\rho_c$	1	2.18×10^{-5}	218	1.59×10^{-5}	8.27×10^{-6}	-4.10	-1.64
$0.15\rho_c$	$1/\sqrt{6}$	1.52×10^{-5}	26	1.27×10^{-5}	9.17×10^{-6}	-0.738	-0.33
$0.15\rho_c$	1	9.74×10^{-6}	788	4.94×10^{-6}	5.31×10^{-7}	-3.0	-0.56
$0.3\rho_c$	$1/\sqrt{6}$	1.08×10^{-5}	138	1.05×10^{-5}	4.99×10^{-6}	-0.71	-0.30
$0.3\rho_c$	1	6.88×10^{-6}	1215	2.64×10^{-6}	-	-2.41	-
$0.6\rho_c$	$1/\sqrt{6}$	7.62×10^{-6}	295	$5.3 \times 10^{-}6$	$2.38 \times 10^{-}6$	-0.65	-0.25
$0.6\rho_c$	1	4.87×10^{-6}	1818	1.22×10^{-6}	-	-1.80	-
ρ_c	$1/\sqrt{6}$	5.9×10^{-6}	452	3.71×10^{-6}	1.18×10^{-6}	-0.60	-0.19
ρ_c	1	3.77×10^{-6}	2418	5.86×10^{-7}	-	-1.32	-

Table 3: For the value of $\Lambda = 16.8$ eV for different values on the background density ρ_∞. The values of $\phi(r)/M_{Pl}$ in this table is taken at the last point for the range of r i.e. in this case when $r = 5000$ kpc. Also here the additional mass M_ϕ gets larger than the virial mass M_{vir} when $\beta = 1$ but again, for higher values of the density it also decreases a little bit. See section [2.3] for further explanation on the negative value on M_ϕ. $\phi(r_{vir})/M_{Pl}$ contributes for all the values of ρ_∞ when $\beta = 1/\sqrt{6}$ and also for $\beta = 1$ until $\rho_\infty = 0.3\rho_c$. Now, it is notable that the value of $\phi(r_{vir})/M_{Pl}$ is very close to the value of ϕ_∞/M_{Pl}. Observe that R_o is negative for the first value of ρ_∞. It means that it ends inside the galaxy cluster and that the coupling do not concour the field potential i.e. the field rolls quckly along its potential.

For this value of Λ, all the five curves will appear in all of the figures below. Still, it is once again for sure that the surrounding density ρ_∞ does not have the same impact on the field profile as the coupling strength β has just by studying the resulting numbers of $\phi(r)/M_{Pl}$ and M_ϕ in Table 3. Also, for $\beta = 1$, the additional mass M_ϕ gets larger than M_{vir} as can be noticed in Figure 12. R_o is taking on a value which is quite small compared to its value for the previous values of Λ and it is also smaller than the virial radius, $R_o < r_{vir}$ for almost all the values, except for the last one when $\rho_\infty = \rho_c$ and $\beta = 1$. This may not come as a surprise after all because a quite dense area with a strong coupling results in a larger transition scale which is going from the inner to the outer solution of the field profile. $\phi(r_{vir})/M_{Pl}$ contributes for all the values of ρ_∞ when $\beta = 1/\sqrt{6}$ and also for $\beta = 1$ at least until $\rho_\infty = 0.3\rho_c$. What is noticeable here is that the value of $\phi(r_{vir})/M_{Pl}$ and ϕ_∞/M_{Pl} is very close to each other.

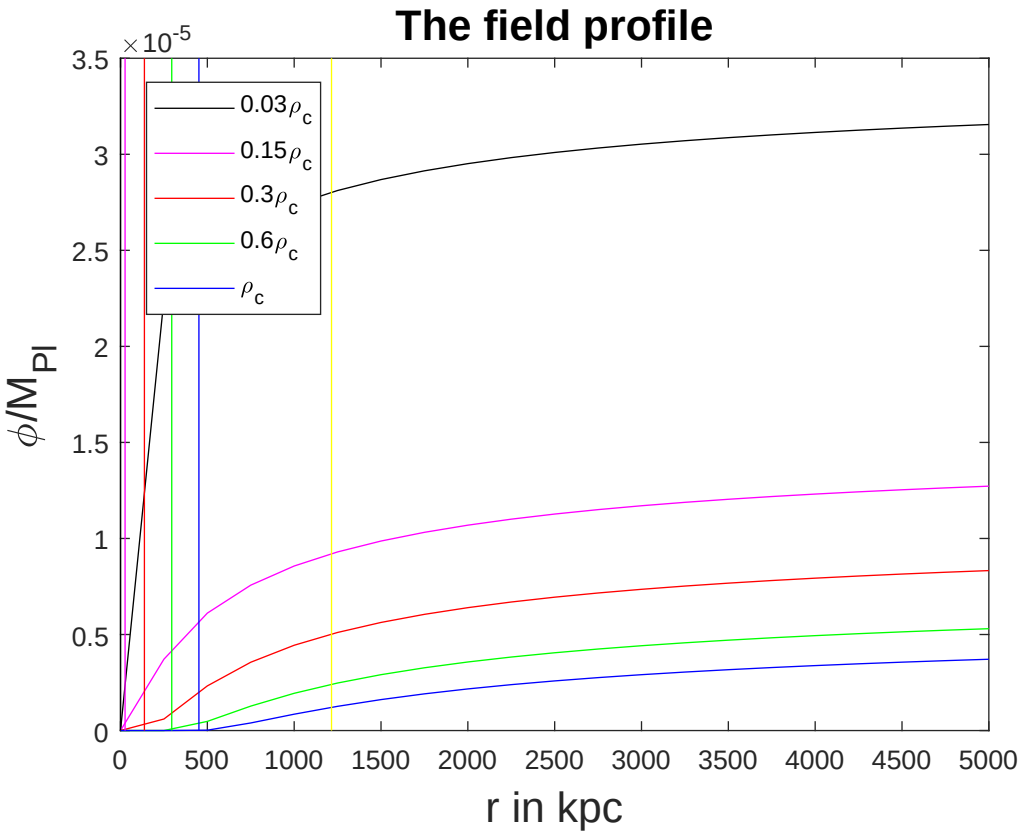

Figure 9: A plot over $\phi(r)/M_{Pl}$ with respect to r ranging from 0 to 5000 kpc for $\Lambda = 16.8$ eV and $\beta = 1/\sqrt{6}$. For this particular value of Λ, all the five curves appear. As usual, the grey curve is when $\rho_\infty = 0.1 \times 0.3\rho_c$ but here its critical radius R_o is vanishing this means that the force is always unscreened. The other four curves have a non-vanishing R_o but grows slowlier than the grey curve. same thing goes for the four other curves but with a much slower increase. The magenta colored curve is for $\rho_\infty = 0.5 \times 0.3\rho_c$ with a belonging magenta colored vertical line for its R_o, the red curve is when $\rho_\infty = 0.3\rho_c$ with a red vertical line for its R_o, the green curve is for $\rho_\infty = 0.6\rho_c$ with a green vertical line for R_o and the blue one is when $\rho_\infty = \rho_c$ with a blue vertical line for its R_o. r_{vir} is at 1215 kpc marked with a yellow vertical line.

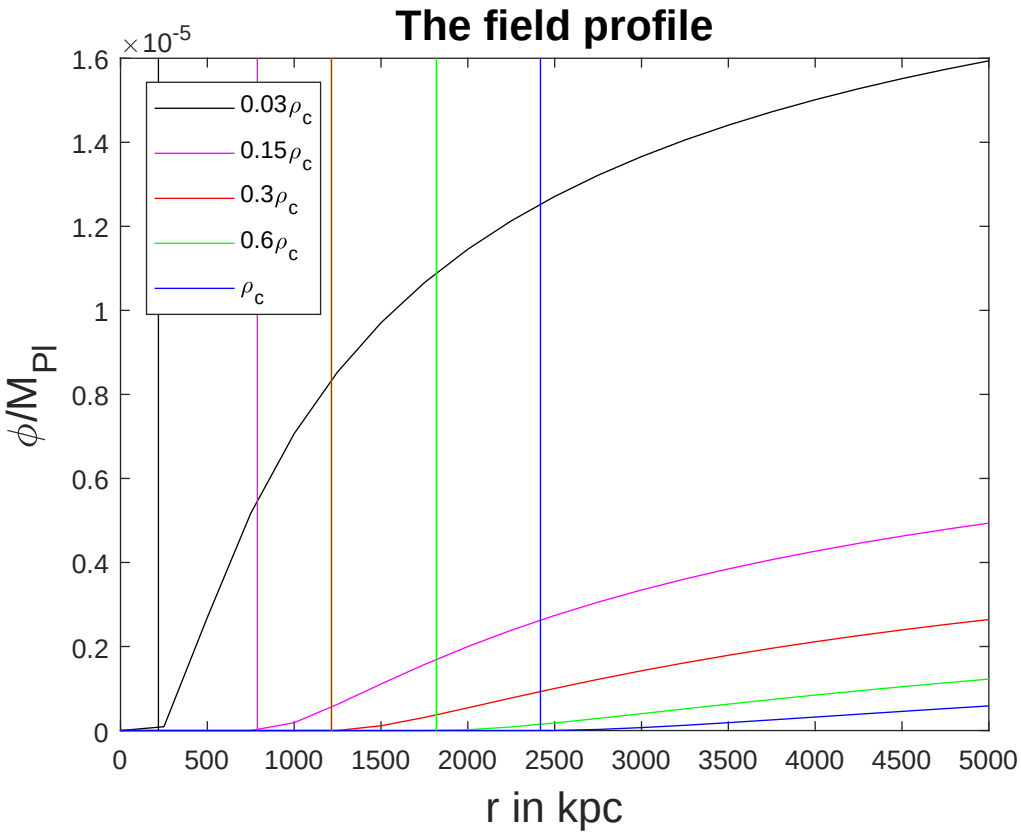

Figure 10: A plot over $\phi(r)/M_{Pl}$ with respect to r ranging from 0 to 5000 kpc for $\Lambda = 16.8$ eV and $\beta = 1$. The difference here is that all of the functions (especially for ρ_∞, Table 3), are barely growing before R_o. The grey curve represents $\rho_\infty = 0.1 \times 0.3\rho_c$ with a vertical grey line marking out its R_o, the magenta coloured curve is for $\rho_\infty = 0.5 \times 0.3\rho_c$ with a belonging magenta coloured vertical line for its R_o, the red curve is when $\rho_\infty = 0.3\rho_c$ with its R_o marked out with a red vertical line, the green curve has a vertical green line marking out the R_o for $\rho_\infty = 0.6\rho_c$ and the blue one is when $\rho_\infty = \rho_c$ with a blue vertical line for its R_o. As usual r_{vir} is at 1215 kpc which is marked out with a yellow vertical line.

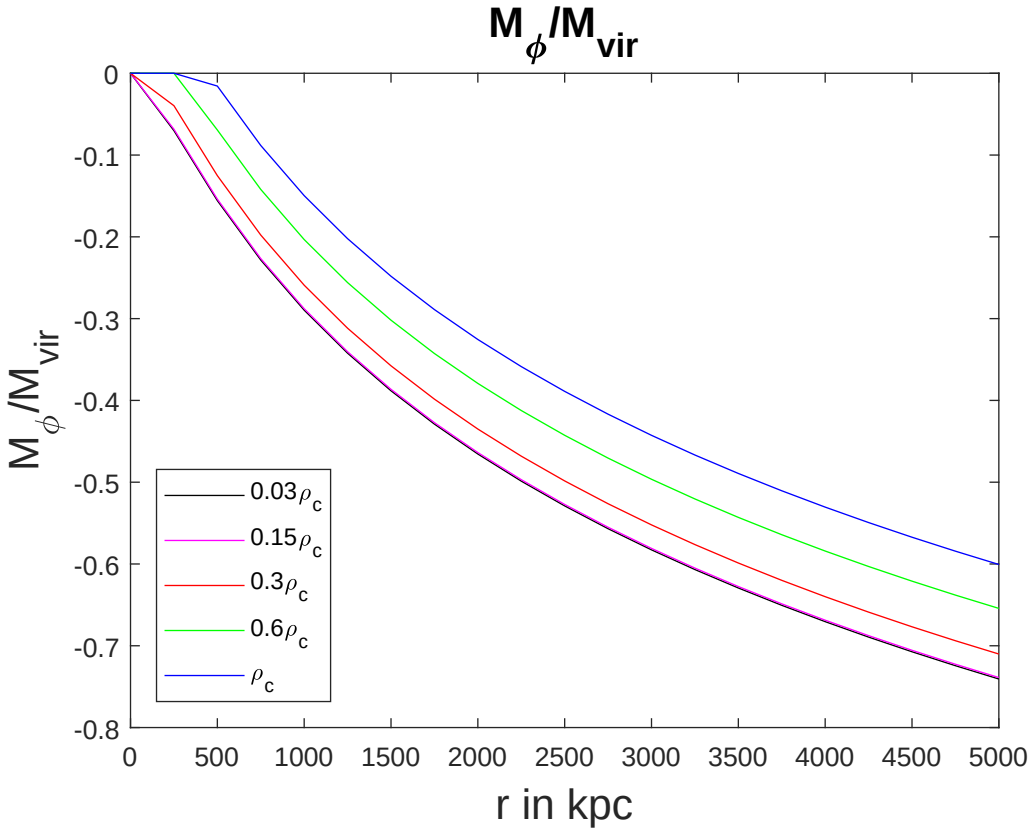

Figure 11: A plot over M_ϕ/M_{vir} with respect to r ranging from 0 to 5000 kpc for $\Lambda = 16.8$ eV and $\beta = 1/\sqrt{6}$. Here the functions are decreasing until R_o and beyond (see Table 3 for each value on R_o). The grey curve is when $\rho_\infty = 0.1 \times 0.3\rho_c$, the magenta coloured curve is for $\rho_\infty = 0.5 \times 0.3\rho_c$, the red curve is when $\rho_\infty = 0.3\rho_c$, the green curve is for $\rho_\infty = 0.6\rho_c$ and the blue one is when $\rho_\infty = \rho_c$. See section 2.3] for more information about the negative value of M_ϕ.

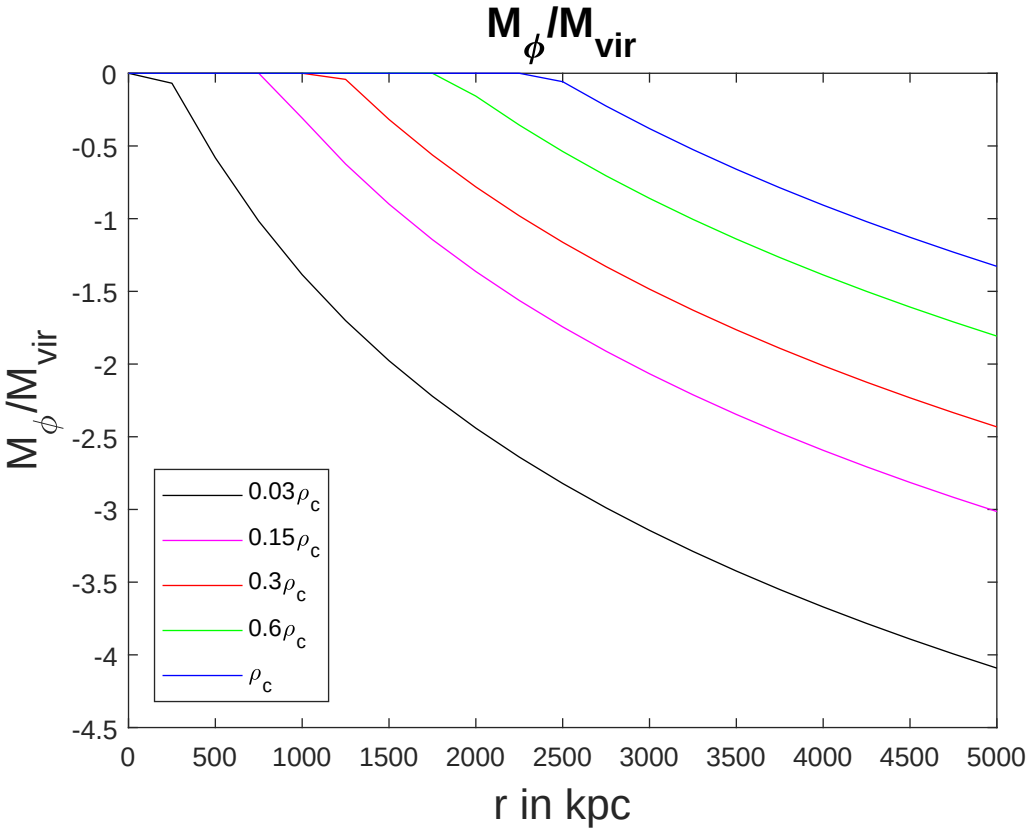

Figure 12: A plot over M_ϕ/M_{vir} with respect to r ranging from 0 to 5000 kpc for $\Lambda = 16.8$ eV and $\beta = 1$. Here the functions barely decrease at all before R_o (see Table 3 for each value of R_o) and there is only a small decrease of the blue curve when the background density is equal to the critical density. As usual, the grey curve is when $\rho_\infty = 0.1 \times 0.3\rho_c$, the magenta coloured curve is for $\rho_\infty = 0.5 \times 0.3\rho_c$, the red curve is when $\rho_\infty = 0.3\rho_c$, the green curve is for $\rho_\infty = 0.6\rho_c$ and the blue one is when $\rho_\infty = \rho_c$ while r_{vir} can be found at 1215 kpc. See section [2.3] for more information about the negative value on M_ϕ.

R_o is determined by $\beta M_{Pl}/\phi_\infty$ where the chameleon field is screened so it means that a small value on ϕ_∞ gives a larger value on R_o and that is the reason the whole cluster can be screened.

The reason why the additional mass M_ϕ is negative is because the fifth force F_ϕ produces an attractive force when the chameleon field couples to the matter fields so it is actually reducing the hydrostatical mass $M_{thermal} + M_\phi$ (compared to the mass in the Newtonian gravity), see section [2.3]. This

means that there will be a deviation between the mass from weak lensing M_{WL} and the mass obtained from gas observations [4].

4 Discussion

The results of the field profile $\phi(r)/M_{Pl}$ and the additional mass M_ϕ are plotted as functions over a distance r in Matlab and presented in figures in section [3]. Some of the result of the critical radius R_o are nonphysical, i.e. zero or negative, especially for higher values of Λ where results can be found in Table 3-Table5. Sometimes R_o also takes on a too large value, i.e. whenever it exceeds 10000 kpc such cases cannot be considered since 10000 kpc is half the average distance between the galaxy clusters and therefore effects from the neighbouring cluster would have to be taken into account this is happening for the lower values of Λ, see Table 1 -2. The larger the values of the background density far out of the galaxy cluster ρ_∞ gave smaller values of the background field profile. For $\Lambda = 4.66$ eV contributions of the field profile and the additional mass were only found for low values of the surrounding density (for $\rho_\infty = 0.1 \times 0.3\rho_c$ up to $\rho_\infty = 0.3\rho_c$) and $\beta = 1/\sqrt{6}$

For $\Lambda = 10$ eV there is a tendency of getting large values of M_ϕ which even exceed the value of the viral mass M_{vir} for low values of ρ_∞ but with $\beta = 1$. This scenario could be an effect of β coupling harder to the matter fields and creating a situation with a heavier contribution from the additional mass and instead the additional mass will decrease for higher values of ρ_∞. This is due to the principle that the force get more screened in denser areas which in turn affects the field profile and the additional mass in a sense that they also get lower value which can be observed in Table 2. When $\Lambda = 16.8$ eV there will be contribution from all the different values of both ρ_∞ and β and the the same tendency as in the previous case can be observed i.e. that M_ϕ is larger than M_{vir} as seen in Table 3 but instead R_o is taking lower values. For $\Lambda = 72.9$ eV, ϕ_∞/M_{Pl} and $\phi(r)/M_{Pl}$ are taking values close to each other while the deviation between them decreases with increasing density but after $\rho_\infty = 0.6\rho_c$ for $\beta = 1$ the value of ϕ_∞ gets slightly larger than $\phi(r)/M_{Pl}$. The same can be seen for $\Lambda = 16.8$ eV for the lower values of ρ_∞ up to a value of when $\rho_\infty = 0.6\rho_c$ for $\beta = 1/\sqrt{6}$. In general, a larger value of Λ gives a higher value of M_ϕ especially for the case for a stronger coupling constant when $\beta = 1$.

The result is compared to the results in paper [21]. In their paper they compare the lensing mass to the dynamical mass M_D which is obtained of observation from velocity dispersion of galaxies. They interpret the dynamical mass as the sum of the weak lensing mass and an additional positive mass in-

ferred from the chameleon's fifth force. There additional mass is comparable to the additional mass M_ϕ obtained in this thesis. For example, considering Figure 11 and Figure 12 for the absolute value of M_ϕ and comparing it with Figure B1 and B2 in their paper, it can be seen that they are qualitatively similar. Both increase similarly for small radii and have an asymptotic behavior for large radii. This confirms the results obtained in this thesis.

The field profile behaves as expected, it is dependent on the surrounding density and the strength of the coupling constant β. Furthermore, it was shown that the chameleon model can at least qualitatively explain the discrepancy between the weak lensing and the hydrostatic mass. To see whether this can also be explained quantitatively, a comparison with observational data would be required.

A Appendix

A.1 The geodesic, FLRW metric and the Ricci tensor

The metric describes the geodesic and how a free falling particle follows the geodesic [12]

$$ds^2 = g_{\mu\nu} dx^\mu dx^\nu. \tag{113}$$

The metric of a flat expanding universe is a Friedman-Lemaitre-Robert-Walker metric.

$$g_{\mu\nu} = diag(-1, a^2(t), a^2(t), a^2(t)) \tag{114}$$

where a is a scale factor which depends on the density. The geodesic equation is:

$$\frac{\mathrm{d}^2 x^\mu}{\mathrm{d}\lambda^2} + \Gamma^\mu_{\alpha\beta} \frac{\mathrm{d}x^\alpha}{\mathrm{d}\lambda} \frac{\mathrm{d}x^\beta}{\mathrm{d}\lambda} = 0 \tag{115}$$

where the Christoffel symbols are obtained from the metric:

$$\Gamma^\mu_{\alpha\beta} = \frac{g^{\mu\nu}}{2} \left[\frac{\partial g_{\alpha\nu}}{\partial x^\beta} + \frac{\partial g_{\beta\nu}}{\partial x^\alpha} - \frac{\partial g_{\alpha\beta}}{\partial x^\nu} \right] \tag{116}$$

$g^{\mu\nu}$ is the inverse metric of $g_{\mu\nu}$ with spatial element $\frac{1}{a^2}$ instead of a^2. So the components of the Christoffel symbols for a flat FLRW metric is: $\Gamma^0_{ij} = \delta_{ij} \dot{a} a, \Gamma^i_{0j} = \Gamma^i_{j0} = \frac{\dot{a}}{a} \delta^i_j$ while the rest of the components are zero. The Ricci tensor is defined as follows:

$$R_{\mu\nu} = \partial_\alpha \Gamma^\alpha_{\mu\nu} - \partial_\nu \Gamma^\alpha_{\mu\alpha} + \Gamma^\alpha_{\beta\alpha} \Gamma^\beta_{\mu\nu} - \Gamma^\alpha_{\beta\nu} \Gamma^\beta_{\mu\alpha} \tag{117}$$

Using the Christoffel symbols obtained earlier where $\mu, \nu = 0$ or $\mu, \nu = i, j$ and the fact that $\delta_i^i = 3$:

$$R_{00} = 3\left(\frac{\ddot{a}}{a}\right), R_{ij} = -\delta_{ij}\Big[2\dot{a}^2 + \ddot{a}a\Big] \tag{118}$$

The Ricci scalar is then obtained by contracting the Ricci tensor:

$$R \equiv g^{\mu\nu}R_{\mu\nu} \tag{119}$$

$$= -R_{00} + \frac{1}{a^2}\delta^{ij}R_{ij} \tag{119}$$

$$= 6\left[\frac{\ddot{a}}{a} - \left(\frac{\dot{a}}{a}\right)^2\right]. \tag{119}$$

A.2 The action

Here the metric g will be evaluated in the action S. Consider the action S:

$$S = \frac{1}{M_{Pl}^2}\int \mathrm{d}^4x\sqrt{-g}\mathcal{R} + S_m \tag{120}$$

Where $\mathcal{R}$ is the Riccii scalar and g is the determinant of the metric $g^{\mu\nu}$ and S_m represent the action of the matter fields. The variation of the action with respect to $g^{\mu\nu}$

$$\delta S = \frac{M_{Pl}^2}{2}\int \mathrm{d}^4x\Big[\delta(\sqrt{-g})g^{\mu\nu}\mathcal{R}_{\mu\nu} + \sqrt{-g}\delta g^{\mu\nu}\mathcal{R}_{\mu\nu} \qquad + \sqrt{-g})g^{\mu\nu}\delta\mathcal{R}_{\mu\nu}\Big] + \delta S_m$$

The last term will vanish because

$$\delta\mathcal{R}_{\mu\nu} = \big(\delta\Gamma^\alpha_{\mu\nu} - \delta\Gamma^\alpha_{\mu\nu}\big)_{;\nu} \tag{120}$$

so that the third term becomes

$$g^{\mu\nu}\delta\mathcal{R}_{\mu\nu} = \big(g^{\mu\nu}\delta\Gamma^\alpha_{\mu\nu} - g^{\mu\alpha}\delta\Gamma^\nu_{\mu\nu}\big)_{;\alpha} \tag{121}$$

plug it back into the action and still only considering the third term

$$\int \mathrm{d}^4x(\sqrt{-g})g^{\mu\nu}\delta\mathcal{R}_{\mu\nu} = \int \mathrm{d}^4x\sqrt{-g}\big(g^{\mu\nu}\delta\Gamma^\alpha_{\mu\nu} - g^{\mu\alpha}\delta\Gamma^\nu_{\mu\nu}\big)_{;\alpha} = 0 \tag{122}$$

So now by using

$$\delta\sqrt{-g} = -\frac{1}{2}\sqrt{-g}g_{\mu\nu}\delta g^{\mu\nu} \tag{123}$$

on the two first terms which are left

$$\delta S = \frac{M_{Pl}^2}{2}\int \mathrm{d}^4x\Big[-\frac{1}{2}\sqrt{-g}g_{\mu\nu}\delta g^{\mu\nu}g^{\mu\nu}\mathcal{R}_{\mu\nu} + \sqrt{-g}\delta g^{\mu\nu}\mathcal{R}_{\mu\nu}\Big] + \delta S_m \tag{124}$$

$$\delta S = \frac{M_{Pl}^2}{2}\int \mathrm{d}^4x\sqrt{-g}\Big[-\frac{1}{2}g_{\mu\nu}g^{\mu\nu}\mathcal{R}_{\mu\nu} + \mathcal{R}_{\mu\nu}\Big]\delta g^{\mu\nu} + \delta S_m \tag{125}$$

and finally the action becomes:

$$\delta S = \frac{M_{Pl}^2}{2}\int \mathrm{d}^4x\sqrt{-g}\Big[\mathcal{R}_{\mu\nu} - \frac{1}{2}g_{\mu\nu}\mathcal{R}\Big]\delta g^{\mu\nu} + \delta S_m. \tag{126}$$

Where the Stress-energy tensor is defined from the variation of S_m [5]:

$$\delta S_m = \frac{1}{2}\int \mathrm{d}^4x\sqrt{-g}T_{\mu\nu}\delta g^{\mu\nu}. \tag{127}$$

A.3 More about the Einstein-Hilbert equation

So now when the action is varied with respect to the metric, the only independent scalars which are produced are the Ricci scalars because with its derivatives not higher than second order, it leads to the simplest Lagrangian so that the action i.e. the Einstein-Hilbert action is then:

$$S_H = -\int \mathrm{d}^4x\sqrt{-g}\mathcal{R} \tag{128}$$

varying the action gives:

$$\delta S_H = -\int \mathrm{d}^4x\sqrt{-g}(\mathcal{R}_{\mu\nu} - \frac{1}{2}\mathcal{R}g_{\mu\nu})\delta g^{\mu\nu} \tag{129}$$

and at stationary point the gravitational part of the action gives :

$$\frac{\delta S_H}{\sqrt{-g}\delta g^{\mu\nu}} = (\mathcal{R}_{\mu\nu} - \frac{1}{2}\mathcal{R}g_{\mu\nu}) = 0. \tag{130}$$

This is the Einstein equation in vacuum. By including the matter action which contains the matter fields, the action then becomes:

$$S = -\frac{M_{Pl}^2 S_H}{2} + S_M = -\frac{S_H}{16\pi G} + S_M \tag{131}$$

the action can now finally written as will:

$$S = -\frac{M_{Pl}^2}{2}\int \mathrm{d}^4x\sqrt{-g}\mathcal{R} + S_M \tag{132}$$

now varying this action:

$$\delta S = -\frac{M_{Pl}^2}{2}\int \mathrm{d}^4x\sqrt{-g}(\mathcal{R}_{\mu\nu} - \frac{1}{2}\mathcal{R}g_{\mu\nu})\delta g^{\mu\nu} + \delta S_M = 0 \tag{133}$$

and at a stationary point:

$$\frac{\delta S}{\sqrt{-g}\delta g^{\mu\nu}} = -\frac{M_{Pl}^2}{2}(\mathcal{R}_{\mu\nu} - \frac{1}{2}\mathcal{R}g_{\mu\nu}) + \frac{\delta S_M}{\sqrt{-g}\delta g^{\mu\nu}} = 0 \tag{134}$$

$$(\mathcal{R}_{\mu\nu} - \frac{1}{2}\mathcal{R}g_{\mu\nu}) = 16\pi G\frac{\delta S_M}{\sqrt{-g}\delta g^{\mu\nu}} \tag{135}$$

and remembering that the Einstein equation is:

$$(R_{\mu\nu} - \frac{1}{2}Rg_{\mu\nu}) = 8\pi G T_{\mu\nu} \tag{136}$$

so from this it is a little bit clearer the stress-energy tensor is [12]:

$$T_{\mu\nu} = \frac{2\delta S_M}{\sqrt{-g}\delta g^{\mu\nu}}. \tag{137}$$

From the action in equation (148)

$$S = \frac{M_{Pl}^2}{2}\int \mathrm{d}^4x\sqrt{-g}(\mathcal{R} + f(\mathcal{R})) + S_m \tag{138}$$

[2]. Lets only considering the $f(\mathcal{R})$ part. The procedure will be the same as above

$$S = \frac{M_{Pl}^2}{2}\int \mathrm{d}^4x\sqrt{-g}f(\mathcal{R}) \tag{139}$$

$$\delta S = \frac{M_{Pl}^2}{2}\int \mathrm{d}^4x\big(\sqrt{-g}\delta f(\mathcal{R}) + f(\mathcal{R})\delta\sqrt{-g}\big) \tag{140}$$

From this lets defining $\partial f(\mathcal{R})/\partial R = F(\mathcal{R})$

$$\delta S = \frac{M_{Pl}^2}{2}\int \mathrm{d}^4x\big(F(\mathcal{R})\delta\mathcal{R}\sqrt{-g} - \frac{1}{2}\sqrt{-g}g_{\mu\nu}\delta g^{\mu\nu}f(\mathcal{R})\big). \tag{141}$$

Remembering that [5]

$$\delta\mathcal{R} = g^{\mu\nu}\mathcal{R}_{\mu\nu} \tag{142}$$

and that

$$\delta\mathcal{R} = \mathcal{R}_{\mu\nu}\delta g^{\mu\nu} + g^{\mu\nu}\delta\mathcal{R}_{\mu\nu}. \tag{143}$$

The procedure now is just like before but with different index and writing out the derivatives:

$$\delta\mathcal{R}_{\mu\nu} = \left(\nabla_\rho\delta\Gamma^\rho_{\mu\nu} - \nabla_\nu\delta\Gamma^\rho_{\mu\rho}\right) \tag{144}$$

and $\delta\Gamma^\rho_{\nu\mu}$ can be rewritten like this:

$$\delta\Gamma^\rho_{\mu\nu} = \frac{1}{2}g^{\rho\alpha}\left(\nabla_\nu\delta g_{\mu\alpha} + \nabla_\mu\delta g_{\nu\alpha} - \nabla_\alpha\delta g_{\mu\nu}\right) \tag{145}$$

$$\delta\Gamma^\rho_{\mu\rho} = \frac{1}{2}g^{\rho\alpha}\left(\nabla_\rho\delta g_{\alpha\mu} + \nabla_\mu\delta g_{\alpha\rho} - \nabla_\alpha\delta g_{\mu\rho}\right) \tag{146}$$

because it is the difference between two connections and therefore should be transforming like a tensor. Plug it back into equation (144):

$$\begin{aligned}\delta\mathcal{R}_{\mu\nu} &= \nabla_\rho\left(\frac{1}{2}g^{\rho\alpha}\left(\nabla_\nu\delta g_{\mu\alpha} + \nabla_\mu\delta g_{\nu\alpha} - \nabla_\alpha\delta g_{\mu\nu}\right)\right) - \\ &\quad \nabla_\nu\left(\frac{1}{2}g^{\rho\alpha}\left(\nabla_\rho\delta g_{\alpha\mu} + \nabla_\mu\delta g_{\alpha\rho} - \nabla_\alpha\delta g_{\mu\rho}\right)\right)\end{aligned} \tag{146}$$

and finally plug it into equation (143)

$$\begin{aligned}\delta\mathcal{R} &= \mathcal{R}_{\mu\nu}\delta g^{\mu\nu} + g^{\mu\nu}\left(\nabla_\rho\left(\frac{1}{2}g^{\rho\alpha}\left(\nabla_\nu\delta g_{\mu\alpha} + \nabla_\mu\delta g_{\nu\alpha} - \nabla_\alpha\delta g_{\mu\nu}\right)\right)\right. \\ &\quad \left.-\nabla_\nu\left(\frac{1}{2}g^{\rho\alpha}\left(\nabla_\rho\delta g_{\alpha\mu} + \nabla_\mu\delta g_{\alpha\rho} - \nabla_\alpha\delta g_{\mu\rho}\right)\right)\right).\end{aligned} \tag{146}$$

This gives the final result

$$\delta\mathcal{R} = \mathcal{R}_{\mu\nu}\delta g^{\mu\nu} + g_{\mu\nu}\Box\delta g^{\mu\nu} - \nabla_\mu\nabla_\nu\delta g^{\mu\nu}. \tag{147}$$

This can be plugged back into the integral in equation (139)

$$\begin{aligned}\delta S &= \frac{M_{Pl}^2}{2}\int \mathrm{d}^4x\left(F(\mathcal{R})\left(\mathcal{R}_{\mu\nu}\delta g^{\mu\nu} + g_{\mu\nu}\Box\delta g^{\mu\nu} - \nabla_\mu\nabla_\nu\delta g^{\mu\nu}\right)\sqrt{-g}\right. \\ &\quad \left.-\frac{1}{2}\sqrt{-g}g_{\mu\nu}\delta g^{\mu\nu}f(\mathcal{R})\right).\end{aligned} \tag{147}$$

$$\delta S = \frac{M_{Pl}^2}{2}\int \mathrm{d}^4x\sqrt{-g}\delta g^{\mu\nu}\Big(F(\mathcal{R})\mathcal{R}_{\mu\nu} + F(\mathcal{R})g_{\mu\nu}\Box - \nabla_\mu\nabla_\nu F(\mathcal{R}) - \frac{1}{2}g_{\mu\nu}f(\mathcal{R})\Big). \tag{147}$$

Finally everything can be put into the integral in equation (138) i.e. the $\mathcal{R}$ -part which is the result from section [A.2] equation (126) combined with the $f(\mathcal{R})$ -part achieved now in equation (148).

$$\delta S = \frac{M_{Pl}^2}{2}\int \mathrm{d}^4x\sqrt{-g}\delta g^{\mu\nu}\Big(\mathcal{R}_{\mu\nu} - \frac{1}{2}g_{\mu\nu}\mathcal{R} + F(\mathcal{R})\mathcal{R}_{\mu\nu} + F(\mathcal{R})g_{\mu\nu}\Box - \nabla_\mu\nabla_\nu F(\mathcal{R}) - \frac{1}{2}g_{\mu\nu}f(\mathcal{R})\Big). \tag{147}$$

The variation is invariant under variation i.e. $\delta S = 0$ this will finally result in the field equation

$$\mathcal{R}_{\mu\nu} - \frac{1}{2}g_{\mu\nu}\mathcal{R} + F(\mathcal{R})\mathcal{R}_{\mu\nu} - \frac{1}{2}g_{\mu\nu}f(\mathcal{R}) + g_{\mu\nu}\Box F(\mathcal{R}) - \nabla_\mu\nabla_\nu F(\mathcal{R}) = \kappa T_{\mu\nu} \tag{147}$$

Where $\kappa = 8G\pi$ [2] and the reduced Planck mass is

$$M_{Pl}^2 = \frac{1}{8\pi G}. \tag{148}$$

A.3.1 Additional part to section [1.6]

We have the action from equation (31) in section [1.6]

$$S = \frac{M_{Pl}^2}{2}\int \mathrm{d}^4x\Phi^{-2}\sqrt{-\tilde{g}}\Phi^2\Big(\tilde{\mathcal{R}} + 3\frac{\Box\Phi}{\Phi} - \frac{9}{2}\big(\frac{\nabla\Phi}{\Phi}\big)^2 - \frac{V(\Phi)}{\Phi^2}\Big) + S_m[\Phi^{-1}\tilde{g}_{\mu\nu}, \psi]$$

First, treat the second term $3\frac{\Box\Phi}{\Phi}$ in the action and chose $\Phi = \mathrm{e}^{2\beta\phi/M_{Pl}}$:

$$\begin{aligned} 3\frac{\Box\Phi}{\Phi} = 3\frac{\Box \mathrm{e}^{2\beta\phi/M_{Pl}}}{\mathrm{e}^{2\beta\phi/M_{Pl}}} &= 3\frac{\partial_\mu(\partial^\mu \mathrm{e}^{2\beta\phi/M_{Pl}})}{\mathrm{e}^{2\beta\phi/M_{Pl}}} \\ &= 3\frac{\left(\frac{\partial_\mu(\frac{2\beta}{M_{Pl}}(\partial^\mu\phi)e^{2\beta\phi/M_{Pl}})}{\mathrm{e}^{2\beta\phi/M_{Pl}}}\right)}{\mathrm{e}^{2\beta\phi/M_{Pl}}} \\ &= 3\frac{\left(\frac{2\beta}{M_{Pl}}\partial_\mu\partial^\mu\phi \mathrm{e}^{2\beta\phi/M_{Pl}} + \frac{4\beta^2}{M_{Pl}^2}\partial_\mu\phi\partial^\mu\phi \mathrm{e}^{2\beta\phi/M_{Pl}}\right)}{\mathrm{e}^{2\beta\phi/M_{Pl}}} \\ &= 3\frac{\left(\frac{2\beta}{M_{Pl}}\Box\phi \mathrm{e}^{2\beta\phi/M_{Pl}} + \frac{4\beta^2}{M_{Pl}^2}(\partial\phi)^2 \mathrm{e}^{2\beta\phi/M_{Pl}}\right)}{\mathrm{e}^{2\beta\phi/M_{Pl}}}. \quad (143) \end{aligned}$$

Now lets treat the third term in equation (31):

$$\begin{aligned} -\frac{9}{2}\big(\frac{\nabla\Phi}{\Phi}\big)^2 = -\frac{9}{2}(\nabla\log\Phi)^2 &= -\frac{9}{2}\nabla^2\big(2\frac{\beta}{M_{Pl}}\big)^2\Phi^2 \\ &= -\frac{9}{2}\big(2\frac{\beta}{M_{Pl}}\big)^2(\partial\phi)^2. \quad (143) \end{aligned}$$

Add these three terms together

$$\begin{aligned} &= \frac{\frac{6\beta}{M_{Pl}}\Box\phi \mathrm{e}^{2\beta\phi/M_{Pl}} + \frac{12\beta^2}{M_{Pl}^2}(\partial\phi)^2\mathrm{e}^{2\beta\phi/M_{Pl}}}{\mathrm{e}^{2\beta\phi/M_{Pl}}} - \frac{9}{2}\big(2\frac{\beta}{M_{Pl}}\big)^2(\partial\phi)^2 \\ &= \frac{6\beta}{M_{Pl}}\Box\phi + \frac{12\beta^2}{M_{Pl}^2}(\partial\phi)^2 - \frac{9}{2}\big(2\frac{\beta}{M_{Pl}}\big)^2 \end{aligned}$$

Using that $\beta^2 = 1/6$

$$\begin{aligned} &= \frac{6\beta}{M_{Pl}}\Box\phi + \frac{2}{M_{Pl}^2}(\partial\phi)^2 - \frac{3}{M_{Pl}^2}(\partial\phi)^2 \\ &= \big(\frac{6\beta}{M_{Pl}}\Box\phi - \frac{(\partial\phi)^2}{M_{Pl}^2}\big). \quad (143) \end{aligned}$$

Plug this back into the action of equation (31) and the $\Box$-term will vanish evaluated at the boundaries -a scalar field and all its derivatives vanish at the boundaries of the integral:

$$S = \int \mathrm{d}^4x\sqrt{-\tilde{g}}\big(\frac{M_{Pl}^2}{2}\tilde{\mathcal{R}} - \frac{1}{2}(\partial\phi)^2 - \tilde{V}(\phi)\big) + S_m[e^{2\beta\phi/M_{Pl}}\tilde{g_{\mu\nu}}, \psi]. \quad (144)$$

A.4 The stress-energy stress tensor

Considering the perfect fluid, defined by a isotropic rest frame pressure P and the rest frame energy density ρ. $T_{\mu\nu}$ are only having diagonal elements. The general form for a perfect fluid is:

$$T^{\mu\nu} = (\rho + P)U^{\mu}U^{\nu} - Pg^{\mu\nu}. \tag{145}$$

Where U^{μ} is the four-velocity vector. This can be reduced to $T^{\mu\nu} = diag(-\rho, g^{ii}P)$ in the rest frame. This must be valid in any frame (it is coordinate-independent because it is a tensor equation). The conservation criterion for the stress-energy tensor is modified in a expanding universe with the result that the covariant derivative vanish

$$\partial_{\mu}T^{\mu}_{\nu} \equiv \frac{\partial T^{\mu}_{\nu}}{\partial x^{\mu}} + \Gamma^{\mu}_{\alpha\mu}T^{\alpha}_{\nu} - \Gamma^{\alpha}_{\nu\alpha}T^{\mu}_{\alpha} \tag{146}$$

$$\partial_{\mu}T^{\mu}_{\nu} = 0 \tag{147}$$

For $\nu = 0, T^{i}_{0}$ vanish by isotropy and using the earlier obtained Christoffel symbols again, gives the continuity equation:

$$\frac{\partial \rho}{\mathrm{d}t} + 3\frac{\dot{a}}{a}(\rho + P) = 0 \tag{148}$$

where the stress-energy tensor metric for a isotropic perfect fluid is:

$$T^{\mu}_{\nu} = \begin{pmatrix} -\rho & 0 & 0 & 0 \\ 0 & P & 0 & 0 \\ 0 & 0 & P & 0 \\ 0 & 0 & 0 & P \end{pmatrix} \tag{149}$$

The Hubble constant is $H = \frac{\dot{a}}{a}$ so by pluggin it into the continuity equation gives:

$$\dot{\rho} + 3H(\rho + P). \tag{150}$$

In order to get the Friedman equation in a flat universe, one only has to consider the time component in the Einstein equation

$$R_{00} - \frac{1}{2}g_{00}R = 8\pi G T_{00} \tag{151}$$

and the Friedman equation for a flat universe then becomes:

$$\left(\frac{\dot{a}}{a}\right)^2 = \frac{8\pi G}{3}\rho \tag{152}$$

This gives a better understanding of how the scale factor a is evolving by time [12].

A.5 The energy density of empty space

In GR the whole energy momentum tensor is the source of the gravitational field. The idea behind a possible vacuum energy arises from that energy normalization matters, only the transition from one energy state to another are measurable matters if there would be a region without gravity. The energy-momentum tensor is locally Lorentz-invariant because the vacuum energy do not have a particular direction. The energy-momentum tensor generalized to an arbitrary frame is:

$$T_{\mu\nu}^{(vac)} = \rho_{vac} g_{\mu\nu}. \tag{153}$$

For the case of vacuum, it look likes a perfect fluid but instead with a pressure with a opposite sign: $P_{vac} = -\rho_{vac}$. The energy momentum tensor is then divided into two components, one is the vacuum part and the other is the matter part $T_{\mu\nu}^{M}$ and the Einstein equation then becomes [12]:

$$R_{\mu\nu} - \frac{1}{2} g_{\mu\nu} R = 8\pi G (T_{\mu\nu}^{M} - \rho_{vac} g_{\mu\nu}). \tag{154}$$

A.6 The action for a scalar field

When deriving the energy-momentum tensor from the action, the partial derivative will be replaced by the covariant derivative for curved space

$$\nabla_\mu T^{\alpha\beta} \equiv \frac{\partial T^{\alpha\beta}}{\partial x^\mu} + \Gamma^\alpha_{\gamma\mu} T^{\gamma\beta} + \Gamma^\beta_{\gamma\mu} T^{\alpha\gamma}. \tag{155}$$

The action for a scalar field is:

$$S_\phi = \int \mathrm{d}^4x \sqrt{-g} \left[\frac{1}{2} g^{\mu\nu} (\nabla_\mu \phi)(\nabla_\nu \phi) - V(\phi) \right] \tag{156}$$

and taking the variation of this action with respect to the metric $g_{\mu\nu}$ gives:

$$\delta S_\phi = \int \mathrm{d}^4x \sqrt{-g} \delta g^{\mu\nu} \left[\frac{1}{2} g^{\mu\nu} (\nabla_\mu \phi)(\nabla_\nu \phi) - \frac{g_{\mu\nu}}{2} \left(g^{\rho\sigma} \nabla_\rho \phi \nabla_\sigma \phi - V(\phi) \right) \right] \tag{156}$$

$$\frac{2\delta S_\phi}{\sqrt{-g}\delta g^{\mu\nu}} = g^{\mu\nu} (\nabla_\mu \phi)(\nabla_\nu \phi) - g_{\mu\nu} \left(\frac{g^{\rho\sigma}}{2} \nabla_\rho \phi \nabla_\sigma \phi - V(\phi) \right). \tag{157}$$

The energy-stress tensor for a scalar field is then derived from the action:

$$T^{\phi}_{\mu\nu} = \nabla_{\mu}\phi\nabla_{\nu}\phi - g_{\mu\nu}\left(\frac{g^{\rho\sigma}}{2}\nabla_{\rho}\phi\nabla_{\sigma}\phi - V(\phi)\right). \tag{158}$$

The covariant derivative is not needed for the case of a homogeneous field and is therefore rewritten as:

$$T^{\phi}_{\mu\nu} = \partial_{\mu}\phi\partial_{\nu}\phi - g_{\mu\nu}\left(\frac{g^{\rho\sigma}}{2}\partial_{\rho}\phi\partial_{\sigma}\phi - V(\phi)\right) \tag{159}$$

and finally the action gives a unique energy-stress tensor for a scalar field [12]:

$$T^{\phi}_{\mu\nu} = \partial_{\mu}\phi\partial_{\nu}\phi - (\frac{1}{2}(\partial\phi)^2 - V(\phi))g_{\mu\nu}. \tag{160}$$

A.7 More about the stress-energy tensor for a scalar field

Scalar tensor theories are mostly formulated in the Jordan frame. So by considering a test particle traveling along the geodesic of the metric, the energy-momentum tensor is covariantly conserved in the Jordan frame and the scalar field is the Einstein equation including a extra scalar but it is the Einstein frame which is a conformal frame. They are called conformal frame because they are connected by conformal transformation. This is because the scalar field coupels non-minimally to the scalar matter fields so that means that the coupling to the scalar field and the scalar curvature is minimal, therefore the Chameleon mechanism is often formulated in the Einstein frame [8].

$T_{\mu\nu}$ is the energy-stress tensor and $\tilde{T}$ is the trace of the matter stress-energy tensor metric in Jordan frame, $\tilde{T} = \tilde{g}^{\mu\nu}\tilde{T}_{\mu\nu}$ but also covariantly conserved $\tilde{\nabla}_{\mu}\tilde{T}^{\mu\nu} = 0$. The metric in the Jordan frame defined as $\tilde{g}_{\mu\nu} = A^2(\phi)g_{\mu\mu}$ and there the conformal factor can be expressed with $A(\phi)$ instead which coupels the matter fields in S_M to ϕ.

The stress-energy tensor is not conserved in the Einstein frame. The action's gravitational part is directed by the Einstein equation:

$$R_{\mu\nu} - \frac{1}{2}Rg_{\mu\nu} = \frac{1}{M^2_{Pl}}(T^{matter}_{\mu\nu} + T^{\phi}_{\mu\nu}). \tag{161}$$

The EOM with the time dependency is:

$$= V^{'}(\phi) - A^3(\phi)A^{'}(\phi)\tilde{T} \tag{162}$$

and $\tilde{T} = A^{-4}T_{matter}$ and plug this into the equation above:

$$-V^{'}(\phi) = -\frac{A^{'}(\phi)}{A(\phi)}T_{matter} \tag{163}$$

Taking the divergence of $T^{\phi}_{\mu\nu}$

$$\nabla_{\mu}T^{\phi}_{\mu\nu} = \nabla^{\mu}\partial_{\mu}\phi\partial_{\nu}\phi - \nabla_{\nu}((\frac{1}{2}(\partial_{\mu}\phi\partial^{\nu}\phi) - V(\phi))) \tag{164}$$

$$\Box\phi\partial_{\nu}\phi + \partial_{\mu}\phi\nabla^{\mu}\partial_{\nu}\phi - \frac{1}{2}\nabla_{\nu}(\partial_{\mu}\phi\partial^{\mu}\phi) - V^{'}(\phi)\nabla_{\nu}\phi \tag{165}$$

$$\Box\phi\partial_{\nu}\phi + \partial_{\mu}\phi\nabla^{\mu}\partial_{\nu}\phi - \frac{1}{2}\nabla_{\nu}\partial_{\mu}\phi\partial^{\mu}\phi - \frac{1}{2}(\partial_{\mu}\phi\nabla_{\nu}\partial^{\mu}\phi) - V^{'}(\phi)\nabla_{\nu}\phi \tag{166}$$

$$\Box\phi\partial_{\nu}\phi + \partial_{\mu}\phi\partial^{\mu}\partial_{\nu}\phi - \partial_{\mu}\phi\partial^{\mu}\partial_{\nu}\phi) - V^{'}(\phi)\partial_{\nu}\phi \tag{167}$$

$$(\Box\phi - V^{'}(\phi))\partial_{\nu}\phi \tag{168}$$

and this can be compared to equation (163) and using equation (161) and the Bianchi identity $\tilde{\nabla}_{\mu}\tilde{G}^{\mu\nu} = 0$

$$T^{matter}_{\mu\nu} = -T^{\phi}_{\mu\nu} \tag{169}$$

$$\nabla_{\mu}T_{matter} = \frac{A^{'}(\phi)}{A(\phi)}T_{matter}\partial_{\nu}\phi \tag{170}$$

Which shows that the stress tensor is not conserved in the Einstein frame [2].

A.8 The effective potential and the effective mass

The field profile is characterized by the mass of the scalar field and it is a product of the effective potential which is locally density dependent. The scalar field will generate a fifth force and due to the fact that the metric couples to the matter fields, a test particle will feel this fifth force. The effective mass gets larger in dense regions and a test particle will feel normal gravity at distances larger than the Compton wavelength m^{-1} because the scalar field will not propagate in dense environments and the fifth force will

be suppressed by the Yukawa potential. The coupling constant β_i is a set of constants which couples ϕ to each matter field Ψ_i. The scalar field will couple to each one of the matter fields with the same universal coupling and can therefore be rewritten as $\nabla^2\phi = \frac{\mathrm{d}V_eff}{\mathrm{d}\phi}$ [6]. That is why the RHS of the equation of motion (EOM) is generalized to an equation which contains the drivative of the effective potential while assuming that there is no time dependency on ϕ in the EOM where the effective potential is a potential to the scalar field and where the scalar field has its minimum $\phi = \phi_{min}$ [8]. As long as both β and ϕ are positive, any run away potential with $\frac{\mathrm{d}V}{\mathrm{d}\phi} < 0$ will give a local minimum for the effective potential so the position of the minimum of the effective potential is dependent on ρ [6]. In other words, by choosing the right values for the potential $V(\phi)$ and for the extra term, the effective potential will find its minimum at some finite field value ϕ_{min}. $\frac{\mathrm{d}\phi_{min}}{\mathrm{d}\rho} < 0$ and ϕ_{min} is assumed to monotonically vary with ρ. The behavior of ϕ is governed by the surrounding density [7]. The local effective mass of the scalar field m^2_{eff} is increasing with increased ρ and therefore the name Chameleon [6]. The effective potentials second derivative is not directly dependent on ρ but in fact it is the minimum of the potential $V(\phi_{min})$ which depends on ρ [8].

A.9 The weak field approximation

As mentioned earlier, the interaction between the matter field $\psi_m^{(i)}$ and the metric takes place via the conformal transformation. The matter field $\psi_m^{(i)}$ is coupling to the metric $g^{(i)}_{\alpha\beta}$ and not the metric $g_{\alpha\beta}$. The geodesics of $g^{(i)}_{\alpha\beta}$ describes the world lines of a free test particle's geodesic [15]. For a flat space-time metric the case is:

$$g_{\mu\nu} = \eta_{\mu\nu} + h_{\mu\nu} \tag{171}$$

where $\eta_{\mu\nu} = diag(-1, 1, 1, 1)$ and it is constant. $h_{\mu\nu}$ is a small correction field with the weak field condition $h_{\mu\nu} << 1$. This expression is flat plus an correction term and h is arbitrary.

$$\frac{\partial g_{\mu\nu}}{\partial x^\rho} = \frac{\partial h_{\mu\nu}}{\partial x^\rho} \tag{172}$$

[12].
In this case with the chameleon field, it is not flat anymore but modified and the conformal transformation is really small. Remembering what was done in section [1.8] with the "extra" term coming from the conformal transformation, calculated the Christoffel symbols and finally the geodesic equation

was obtained:

$$\ddot{x}^{\lambda} + \Gamma^{\lambda}_{\alpha\beta}\dot{x}^{\alpha}\dot{x}^{\beta} = -\frac{\beta}{M_{Pl}} g^{\rho\lambda}\partial_{\rho}\phi \tag{173}$$

Now, consider the perturbed Jordan frame metric [18]:

$$d\tilde{s}^2 = \tilde{a}^2(\eta)\big(-(1+2\phi_N)d^2\eta + (1-2\phi_N)d^i x d^j x\big). \tag{174}$$

Here η is the conformal time and $\tilde{a}$ is the scale factor in the Jordan frame; $\tilde{a} = a\Omega$ where $\Omega = e^{\beta\phi/M_{Pl}}$. ϕ_N is the perturbation of the scalar metric which can be related to the Newtonian gravitational potential $\Phi = \phi_N + \frac{2\beta\phi}{M_{Pl}}$. This metric can be expanded when $\phi_N \ll M_{Pl}$

$$d\tilde{s}^2 = \tilde{a}^2(\eta)\big(-(1+2\phi_N + \frac{2\beta\phi}{M_{Pl}})d^2\eta + (1-2\phi_N + \frac{2\beta\phi}{M_{Pl}})d^i x d^j x\big). \tag{175}$$

So the geodesic of the particle i.e. its trajectory will be affected when the particle couple to gravity because the chameleon will contribute to the Newtonian gravitational potential [18]. Lets go back to the flat case with $g_{00} = -(1+2\Phi)$, this mediates a criteria for determining a weak field $h_{00} \ll \eta_{00} \rightarrow \Phi \ll 1$ [12]. Assuming that $\phi_N \ll 1$ [18] and that $h_{\mu\nu}$ can may be identified as the extra term i.e. $h_{\mu\nu} \simeq \frac{\beta}{M_{Pl}}\phi$ and using the condition $h_{\mu\nu} << 1$ leading to $\frac{\beta}{M_{Pl}}\phi << 1$ and $\beta\phi << M_{Pl}$ [12].

A.10 The field profile of a massive compact object

This section is only treating an analytical approach in how the chameleon mechanism works in more detail. The method used in this thesis for the field profile $\phi(r)$ of the galaxy cluster is treated in section [2].

In order to get a better understanding of the theory behind the chameleon force, also called the fifth force, F_{ϕ} which is suppressed in high density regions. Then, it could be convenient to get a picture of how the so called thin-shell model, often used in chameleon theory, actually works [2]. The thin-shell model is based on the theory about considering a massive compact object containing a core with a surrounding thin-shell. The reason for building up such a model will be considered in this section, step by step, showing how the fifth force which is a product of the chameleon field's interaction with matter will get screened within the core of the massive object due to its density dependent mass discussed earlier in section [1.9] but also how the thin-shell will be the only contribution to the massive object's field profile

outside its surface and beyond. This is done by deriving an approximate solution for ϕ in order to get the field profile which dependence on the object as well as its surrounding.
So to simplify the problem whit a compact object, it can be treated as a static spherically-symmetric body with a homogeneous density where $\rho(r) = \rho_o$, a radius R_o and a mass $M_o = \frac{4\pi R_o^3 \rho_o}{3}$ situated in a homogeneous background ρ_∞ and where the index c is referring to the compact object [1].
The left hand side of Poisson's equation (62) can be rewritten in spherical coordinates

$$\frac{\mathrm{d}^2\phi}{\mathrm{d}r^2} + \frac{2\mathrm{d}\phi}{r\mathrm{d}r} = V^{'}(\phi) + \frac{\beta}{M_{Pl}}\rho \mathrm{e}^{\frac{\beta\phi}{M_{Pl}}} \tag{176}$$

$$\rho(r) = \begin{cases} \rho_o & \mathrm{r} < R_o \\ \rho_\infty & \mathrm{r} > R_o \end{cases} \tag{177}$$

and ϕ_o is restricted to the interior of object while ϕ_∞ is the scalar field outside the object when $r > R_o$ and they are both minimizing their particular effective potential.
This is a second order differential equation which requires two boundary conditions: The first condition must be regular at the origin i.e. $\frac{\mathrm{d}\phi}{\mathrm{d}r} = 0$ at $r = 0$. The second condition is when $\phi \to \phi_\infty$ for $r \to \infty$ [1].
The field profile outside the object but still within a Compton wavelength m^{-1} from the surface will take the form $1/r$ because the field is assumed to always be close to the values that minimize the effective potential. $\phi \simeq \frac{A}{r} + B$ between $R_o < r < m_\infty^{-1}$.
The constants A and B are given by the boundary conditions. $\phi \to \phi_\infty$ gives that $B = \phi_\infty$ and $\phi(R_o) = \phi_o$ gives $A = -R_o(\phi_\infty - \phi_o)$. The solution for the exterior field then becomes:

$$\phi \simeq -\frac{R_o}{r}(\phi_\infty - \phi_o) + \phi_\infty. \tag{178}$$

There will be a kind of "bump" when going from the inside to the outside of the object's surface because the density is going from from ρ_o to ρ_∞ and $\rho_o \gg \rho_\infty$. Therefore, a parallel to electrostatics can be done. Due to the fact that Laplace's equation $\nabla^2\phi \simeq 0$, is approximately valid inside as well as outside the source and it can be seen as a conducting sphere with a thin-shell and a thickness ΔR_o while the chameleon plays the role as a charge near the surface of the source. The surface charge density would then be

$\frac{\beta\rho\Delta R_o}{M_{Pl}}$ and it will avoid the discontinuity in the field gradient when going from inside to the outside of the object.

$$\frac{\mathrm{d}\phi}{\mathrm{d}r} = \frac{\beta\rho}{M_{Pl}}\Delta R_o. \tag{179}$$

[2]

Furthermore, the shell is divided into small volume elements dV where each of the these $dV : s$ contributes to the scalar field ϕ and by summing over all the volume elements within the shell with thickness ΔR the exterior solution for the field profile is obtained [1]. The thickness of a thin-shell is then obtained by taking the derivative of equation (178) with respect to r:

$$\frac{\mathrm{d}\phi}{\mathrm{d}r} = \frac{{R_o}^2}{r}\left(\phi_\infty - \phi_o\right) \tag{180}$$

and then combining it with equation (179) but also considering that the density here is $\rho = \rho_o$ which is extracted from the mass M_o. Solving out ρ then gives $\rho_o = \frac{3M_c}{4\pi R_o^3}$ and finally the shell-thickness is obtained:

$$\frac{\Delta R_o}{R_o} = \frac{\beta 4\pi M_{Pl} R_o}{3\beta M_o}(\phi_\infty - \phi_o) \tag{181}$$

and using that the gravitational potential is $\Phi = \frac{M}{8\pi M_{Pl}^2 R_o}$ [2]:

$$\frac{\Delta R_o}{R_o} = \frac{\phi_\infty - \phi_o}{6\beta M_{Pl}\Phi}. \tag{182}$$

One can think about it like this: The chameleon will minimize the effective potential for the interior density deep inside the massive object [2] where the mass of the chameleon is large [1]. Every volume element dV inside the object i.e. within its core is in proportion to $e^{-m_c\tilde{r}}$ i.e. they get exponentially suppressed [1]. This is the reason why it is convenient to use a screened Coloumb potential -that will say, a Yukawa potential which is suppressing the contribution from the core of the object. The only contribution to the exterior field profile comes from the shell [2].
Therefore, the exterior field profile for a massive object can be written down by also including the Yukawa potential $V_Y = -g^2\frac{e^{kmr}}{r}$ where g is the magnitude of the scaling factor or just the amplitude of the field [3]. Considering that as well as summing over all the elements within the shell gives the following field profile:

$$\phi(r > R_o) \simeq -\frac{3\beta}{4\pi M_{Pl}}\frac{\Delta R_o}{R_o}\frac{M e^{-m_\infty(r-R_o)}}{r} + \phi_\infty \tag{183}$$

for the condition $\frac{\Delta R_o}{R_o} \ll 1$ where r is the distance from the center of the object. This means that the shell is thin and the condition comes from the weak field approximation where $\frac{\beta\phi}{M_{Pl}} \ll 1$ treated in the previous section [A.10]. This can be directly linked by looking at equation (182) and with the condition $\frac{\Delta R_o}{R_o} \ll 1$:

$$\frac{\phi}{\beta M_{Pl}} \ll \tag{184}$$

to get the condition $\frac{\beta\phi}{M_{Pl}} \ll 1$ one just have to multiply with $1/\beta^2$:

$$\frac{\phi}{\beta M_{Pl}} = \frac{1}{\beta^2}\frac{\beta\phi}{M_{Pl}} \ll \frac{1}{\beta^2} \tag{185}$$

This means that if the weak field approximation is fulfilled then the thin-shell model will also be valid.

For a small object ($\frac{\Delta R_o}{R_o} > 1$) which do not have a thin-shell is the same as above but just without the thin-shell factor [1]:

$$\phi(r > R_o) \simeq -\frac{3\beta}{4\pi M_{Pl}}\frac{M\mathrm{e}^{-m_\infty(r-R_o)}}{r}. \tag{186}$$

To summarize this in a simple way would be to say that the chameleon field only couples to a thin-shell just underneath the surface of the object while the ordinary gravitation couples to the whole object's mass M_o. As a consequence of that, the chameleon force will be suppressed on a test mass outside the object in comparison to the gravitational force [2].

A.11 Dimension conversion of the resulting plots

The dimension conversion used for the plots made in Matlab.

$$1pc = 3.086 \times 10^{16} m \tag{187}$$

But all the distances are in kpc:

$$1kpc = 3.086 \times 10^{19} m \tag{188}$$

$$1kpc^3 = 2.94 \times 10^{58} m^3 \tag{189}$$

In natural units:

$$1eV^{-1} = 1.97 \times 10^{-7} m \rightarrow m = \frac{1}{1.97 \times 10^{-7} eV} \tag{190}$$

$1kpc$ in natural units:

$$1kpc = \frac{3.086 \times 10^{19}}{1.97 \times 10^{-7}} eV^{-1} \approx 1.57 \times 10^{26} eV^{-1} \tag{191}$$

$$1eV^{-3} = 7.65 \times 10^{-21} m^3 \tag{192}$$

$$1kpc^3 = \frac{2.94 \times 10^{58}}{7.65 \times 10^{-21}} eV^{-3} = 3.87 \times 10^{78} eV^{-3} \tag{193}$$

$M_{sol} = 1.989 \times 10^{30}$ kg $= \frac{1.989 \times 10^{30}}{1.78 \times 10^{-36}}$ eV $= 1.12 \times 10^{66}$ eV. The reduced Planck mass M_{Pl} in solar masses are:

$$M_{Pl} = 4.341 \times 10^{-9} kg = \frac{4.341 \times 10^{-9}}{1.989 \times 10^{30}} M_{sol} = 2.18 \times 10^{-39} M_{sol} \tag{194}$$

and in eV:

$$M_{Pl} = 2.44 \times 10^{27} eV. \tag{195}$$

$\Lambda^{n+4} = (eV)^{n+4}$, β is dimensionless and only considering the dimensions in natural units in eV gives:

$$\phi_s = \big(\frac{n(eV)^{n+4}(eV)}{\beta(eV^4)}\big)^{1/(n+1)} = (\frac{eV^{n+5}}{eV^4})^{1/(n+1)} = eV \tag{196}$$

and the same goes for ϕ_∞.

Everything is kept in eV in the Matlab code. r is plotted in kpc which for simplicity is done in the plot function, the same goes for $\phi(r)$ which is plotted as $\phi(r)/M_{Pl}$ i.e. dimensionless and the additional mass M_ϕ is plotted as M_ϕ/M_{vir} to get an estimation of how large the additional mass is compared to the virial mass.

References

[1] J. Khoury and A. Weltman, Chameleon cosmology, Phys. Rev. D **69** (2004) 044026 doi:10.1103/PhysRevD.69.044026 [astro-ph/0309411].

[2] A. Joyce, B. Jain, J. Khoury and M. Trodden, Beyond the Cosmological Standard Model, Phys. Rept. **568** (2015) 1 doi:10.1016/j.physrep.2014.12.002 [arXiv:1407.0059 [astro-ph.CO]].

[3] H. Yukawa, On the Interaction of Elementary Particles I, Proc. Phys. Math. Soc. Jap. **17** (1935) 48 [Prog. Theor. Phys. Suppl. **1** 1]. doi:10.1143/PTPS.1.1

[4] A. Terukina, L. Lombriser, K. Yamamoto, D. Bacon, K. Koyama and R. C. Nichol, Testing chameleon gravity with the Coma cluster, JCAP **1404** (2014) 013 doi:10.1088/1475-7516/2014/04/013 [arXiv:1312.5083 [astro-ph.CO]].

[5] Luca Amendola and Shinji Tsujikawa, Dark Energy. Theory and observations, Cambridge University Press, 2010

[6] Timothy Clifton, Pedro G. Ferreira, Antonio Padilla and Constantinos Skordis, Modified Gravity and Cosmology, Phys. Rept. **513**, 1 (2012) doi:10.1016/j.physrep.2012.01.001 [arXiv:1106.2476 [astro-ph.CO]].

[7] Justin Khoury, Chameleon Field Theory, Class. Quant. Grav. **30** (2013) 214004 doi:10.1088/0264-9381/30/21/214004 [arXiv:1306.4326 [astro-ph.CO]].

[8] Kazuya Koyama, Cosmological Tests of Modified Gravity, Rept. Prog. Phys. **79** (2016) no.4, 046902 doi:10.1088/0034-4885/79/4/046902 [arXiv:1504.04623 [astro-ph.CO]].

[9] David Tong, Lectures on Quantum Field Theory, http://www.damtp.cam.ac.uk/user/tong/qft/one.pdf University of Cambridge

[10] Marieke Postma and Marco Volponi, Equivalence of the Einstein and Jordan frames, Phys. Rev. D **90** (2014) no.10, 103516 doi:10.1103/PhysRevD.90.103516 [arXiv:1407.6874 [astro-ph.CO]].

[11] Weisstein, Eric W., Euler-Lagrange Differential Equation, From MathWorld–A Wolfram Web Resource, http://mathworld.wolfram.com/Euler-LagrangeDifferentialEquation.html accessed on 31 March 2018 at 13:45

[12] Ta-Pei Cheng, Relativity, Gravitation and cosmology. A Basic Introduction, second edition, Oxford University press, 2010

[13] P. J. E. Peebles and Bharat Ratra, The Cosmological Constant and Dark Energy, Rev. Mod. Phys. **75** (2003) 559 doi:10.1103/RevModPhys.75.559 [astro-ph/0207347].

[14] P. Bintruy, Models of Dynamic Supersymmetry Breaking and Quintessence, Phys. Rev. D **60** (1999) 063502 doi:10.1103/PhysRevD.60.063502 [hep-ph/9810553].

[15] Andrea Zanzi, Chameleon theories: a short review, Universe **1** (2015) no.3, 446 doi:10.3390/universe1030446 [arXiv:1602.03869 [gr-qc]].

[16] Thomas P. Sotiriou, f(R) gravity and scalar-tensor theory, Class. Quant. Grav. **23** (2006) 5117 doi:10.1088/0264-9381/23/17/003 [gr-qc/0604028].

[17] Julio F. Navarro, Carlos S. Frenk, Simon D.M. White, A Universal Density Profile from Hierarchical Clustering, Astrophys. J. **490** (1997) 493 doi:10.1086/304888 [astro-ph/9611107].

[18] Ph. Brax, R. Rosenfeld, D. A. Steer, Spherical Collapse in Chameleon Models, JCAP **1008** (2010) 033 doi:10.1088/1475-7516/2010/08/033 [arXiv:1005.2051 [astro-ph.CO]].

[19] R. Pourhasan, N. Afshordi, R.B. Mann, A.C. Davis Chameleon Gravity, Electrostatics, and Kinematics in the Outer Galaxy JCAP **1112** (2011) 005 doi:10.1088/1475-7516/2011/12/005 [arXiv:1109.0538 [astro-ph.CO]].

[20] P.J. Steinhardt, L. Wang, I. Zlatev Cosmological tracking solutions Phys. Rev. D **59** (1999) 123504 doi:10.1103/PhysRevD.59.123504 [astro-ph/9812313].

[21] Gong-Bo Zhao, Baojiu Li, Kazuya Koyama Testing General Relativity using the Environmental Dependence of Dark Matter Halos Phys. Rev. Lett. **107** (2011) 071303 doi:10.1103/PhysRevLett.107.071303 [arXiv:1105.0922 [astro-ph.CO]].

[22] NASA / JPL-Caltech / L. Jenkins (GSFC) - http://www.spitzer.caltech.edu/images/1803-ssc2007-10a1-Dwarf-Galaxies-in-the-Coma-Cluster Original work of NASA - public domain accessed on 18 September 2018 at 17:32

[23] C. Burrage and J. Sakstein, A Compendium of Chameleon Constraints, JCAP **1611** (2016) no.11, 045 doi:10.1088/1475-7516/2016/11/045 [arXiv:1609.01192 [astro-ph.CO]].